

Bayesian Empirical Bayes: Simultaneous Inference from Probabilistic Symmetries

Bohan Wu¹Eli N. Weinstein²David M. Blei^{1,3}

December 23, 2025

Abstract

Empirical Bayes (EB) improves the accuracy of simultaneous inference “by learning from the experience of others” (Efron, 2012). Classical EB theory focuses on latent variables that are iid draws from a fitted prior (Efron, 2019). Modern applications, however, feature complex structure, like arrays, spatial processes, or covariates. How can we apply EB ideas to these settings? We propose a generalized approach to empirical Bayes based on the notion of *probabilistic symmetry*. Our method pairs a simultaneous inference problem—with an unknown prior—to a symmetry assumption on the joint distribution of the latent variables. Each symmetry implies an ergodic decomposition, which we use to derive a corresponding empirical Bayes method. We call this method *Bayesian empirical Bayes* (BEB). We show how BEB recovers the classical methods of empirical Bayes, which implicitly assume exchangeability. We then use it to extend EB to other probabilistic symmetries: (i) EB matrix recovery for arrays and graphs; (ii) covariate-assisted EB for conditional data; (iii) EB spatial regression under shift invariance. We develop scalable algorithms based on variational inference and neural networks. In simulations, BEB outperforms existing approaches to denoising arrays and spatial data. On real data, we demonstrate BEB by denoising a cancer gene-expression matrix and analyzing spatial air-quality data from New York City.

1 Introduction

Empirical Bayes (EB) is about *simultaneous posterior inference*. We observe related data x_1, \dots, x_n , where each data point is associated with a latent variable z_i , and assumed drawn from $x_i \sim p(x|z_i)$. The form of the conditional likelihood is known. The goal of EB is to use Bayesian inference to estimate all the z_i together (Robbins, 1956; Efron, 2015b, 2019).

In a traditional Bayesian analysis, we specify a prior $z_i \sim g(z)$ and compute the posteriors $p(z_i|x_i)$. But in EB, we treat the prior $g(z)$ as *unknown* and we estimate it from the data. EB

¹Department of Statistics, Columbia University, New York, NY

²Department of Chemistry, Technical University of Denmark, Denmark

³Department of Computer Science, Columbia University, New York, NY

Contact: bw2766@columbia.edu, enawe@dtu.dk, david.blei@columbia.edu

thus blends Bayesian and frequentist thinking: we reason in a frequentist way about the prior in order to form a collection of Bayesian estimates.

The classical approach to EB assumes $z_1, \dots, z_n \stackrel{iid}{\sim} g$ and estimates \hat{g} so that the marginal distribution of x maximizes the likelihood of the data. In the EB nomenclature, this is known as “g-modeling” (Efron, 2014). Once the prior is fit, we calculate the posteriors $p(z_i | x_i, \hat{g})$ to estimate the latent variables. Through the fitted prior, EB connects all n inferences: information from each observation improves all the others.

The assumption $z_1, \dots, z_n \stackrel{iid}{\sim} g$ is central to EB thinking. It says that the latent variables share a common prior, which justifies the EB procedure. But many modern datasets violate this iid assumption. Latent variables may come in rows and columns, they may lie on a spatial or temporal grid, or they may depend on known covariates. While these settings clearly violate the iid assumption, they still exhibit symmetries that tie the latent variables together. In this paper, we develop a general way to use such probabilistic symmetries to extend EB to non-iid settings.

Stepping back, the assumption that z_1, \dots, z_n are iid from g is a special case of a broader principle: *exchangeability*. If the joint distribution of the latent variables is invariant to permutations, then—under mild conditions—it can be viewed as part of an infinitely exchangeable sequence. The iid structure then arises through de Finetti’s famous representation theorem (Finetti, 1929). It states that any exchangeable sequence can be written as a mixture of iid laws,

$$p(z_1, \dots, z_n) = \int \left[\prod_{i=1}^n p(z_i | g) \right] d\mu(g), \quad (1)$$

where g is a probability distribution on \mathcal{L} and μ is a distribution over such distributions. De Finetti’s result is important because it connects a symmetry assumption—namely, exchangeability—to classical Bayesian reasoning (Savage, 1954; Robert, 2007). If the z_i ’s are exchangeable, then the prior g appears as the latent variable that renders the z_i conditionally independent.

Our insight is that empirical Bayes uses the same hierarchical structure as in Eq. 1, where z_i are conditionally iid given g . However, in place of integration with respect to μ , EB substitutes a fitted value \hat{g} obtained from data. Seen through de Finetti’s theorem, we can view EB as a Bayesian inference under exchangeability, but with the mixing distribution collapsed to a point estimate.

Using this perspective, we extend classical EB by relaxing its exchangeability assumption to other probabilistic symmetries. Latent variables often have structure, such as being organized in an array or indexed by space or time. Such settings are not fully exchangeable, but they may satisfy weaker invariances. An array may be invariant to permutations of its rows and columns; a spatial process may be invariant to shifts in location (Kallenberg, 2005). Each symmetry has an analogue of de Finetti’s representation theorem. We will use these representation theorems to extend EB to non-iid settings.

We call our approach *Bayesian empirical Bayes* (BEB). We begin with a dataset \mathbf{x} and an assumed probabilistic symmetry. We posit that each observation arises from a known likelihood conditioned on a local latent variable $p(x_i | z_i)$, and our goal is to infer all z_i simultaneously. The key idea is that our assumed symmetry implies an *ergodic decomposition* of the prior, i.e., a generalization of de Finetti’s theorem (Orbanz and Roy, 2015). Specifically, if the latent variables are invariant under a group Φ acting on its index set, then their joint distribution admits the form

$$p(\mathbf{z}) = \int p(\mathbf{z} | g) d\mu(g), \quad (2)$$

where g indexes the Φ -ergodic family. The chosen symmetry determines the form of g and the conditional distribution $p(\mathbf{z} | g)$.

Following the EB recipe, we fit g by maximum marginal likelihood under the expanded model $p(\mathbf{z}, \mathbf{x})$,

$$\hat{g} \in \arg \max_g \log \int p(\mathbf{x} | \mathbf{z}) p(\mathbf{z} | g) d\mathbf{z}. \quad (3)$$

Finally, we use \hat{g} to compute the empirical Bayes posteriors $p(z_i | x_i, \hat{g})$. In practice, we can use approximate posterior inference both to fit \hat{g} and estimate $p(z_i | x_i, \hat{g})$.

We illustrate BEB in several data analysis settings. For array data, the relevant symmetry is separate or joint exchangeability, and the ergodic decomposition is given by the Aldous-Hoover theorem (Aldous, 2006). The invariant variable g is a measurable function on $[0, 1]^3$, which we parameterize with a neural network. For spatial data, the relevant symmetry is shift invariance, and we can flexibly model g with stationary ergodic Gaussian processes. In both settings, we can additionally condition on covariates and derive covariate-dependent EB procedures.

Thus, Bayesian empirical Bayes produces a generalization of EB to any probabilistic symmetry. The invariant variable g replaces the classical prior, and the ergodic decomposition supplies the structure needed for inference.

The rest of the paper is organized as follows. § 2 introduces the modeling assumptions and the general methodology of Bayesian empirical Bayes. § 3 develops new inference methods from Bayesian EB principles in three settings: the classical normal sequence model, empirical Bayes matrix recovery, and empirical Bayes spatial regression. For normal means, we show that Bayesian EB with an exchangeable sequence model recovers the nonparametric maximum-likelihood method of Efron (2015a). For the latter two, we derive new EB procedures based on alternative invariances-joint/separate/relative exchangeability for matrices and stationarity for spatio-temporal data. § 4 evaluates these methods in simulation studies. § 5 applies them to real datasets. § 6 concludes with discussion and future directions. Detailed algorithms for our inference procedures and all technical proofs appear in the Appendix.

1.1 Related Work

Empirical Bayes (EB) dates back to the seminal works of [Robbins \(1951, 1956\)](#) and has been developed in both parametric and nonparametric forms ([Efron and Morris, 1971, 1976](#); [Efron et al., 2001](#); [Brown and Greenshtein, 2009](#); [Jiang and Zhang, 2009](#); [Efron, 2011, 2012, 2014, 2015a, 2024](#); [Soloff et al., 2025](#); [Ignatiadis and Wager, 2022](#); [Yang et al., 2024](#)). Much of the nonparametric theory centers on normal and Poisson sequence models. For normal means, [Efron \(2015b\)](#) surveys frequentist assessments of EB estimators and [Efron \(2019\)](#) surveys oracle–Bayes viewpoints. Beyond g-modeling (modeling the prior), [Efron \(2014\)](#) described an alternative EB approach via f -modeling, which models the marginal data distribution; a key tool is Tweedie’s formula, linking the posterior mean to the derivative of the log marginal density. For the f -modeling methods, [Saremi and Hyvärinen \(2019\)](#) and [Ghosh et al. \(2025\)](#) obtain nonparametric EB estimators using flexible score functions, by minimizing the score-matching loss. EB also underpins large-scale multiple testing ([Efron, 2012](#); [Stephens, 2017](#); [Ignatiadis and Huber, 2021](#)). While it is impossible to exhaust the works on empirical Bayes for the normal sequence model, we refer to [Ignatiadis and Sen \(2025a\)](#) for a recent textbook overview. In this work we focus on g-modeling and extend it beyond the iid prior setting to accommodate general invariant latent structures.

Nonparametric EB methods for non-sequence models have only appeared more recently. In high-dimensional linear models and variable selection, variational EB methods—such as SuSiE and related procedures—learn a nonparametric prior over coefficients ([Carbonetto and Stephens, 2012](#); [Wang et al., 2020](#); [Kim et al., 2024](#)). The prior is exchangeable with respect to covariates ([Trippé et al., 2021](#)). The theoretical properties of these methods are beginning to be understood ([Mukherjee et al., 2023](#); [Fan et al., 2023](#)). For low-rank matrices, empirical Bayes matrix factorization and EB–PCA fit learned shrinkage priors for loadings and scores via approximate inference ([Wang and Stephens, 2021](#); [Zhong et al., 2022](#); [Denault et al., 2025](#)). These new developments share the theme of fitting shared priors for latent variables to structure the borrowing of information. Inspired by this line of work, we provide a unified framework for inferring many latent variables by learning a shared latent structure defined by probabilistic symmetries. This invariance-based perspective enables systematic extensions of EB methods.

From a Bayesian perspective, EB concerns approximating a full Bayesian posterior by a point estimate of the hyperparameter (Ch. 5.6.4 of ([Bernardo and Smith, 1994](#))) and is closely connected to hierarchical Bayes ([Lindley and Smith, 1972](#); [Good, 1992](#)). [Deely and Lindley \(1981\)](#) compare the statistical performance of parametric empirical Bayes and hierarchical Bayes on simultaneous inference problems. One can place additional layers of priors on EB hyperparameters; for example, [Kass and Steffey \(1989\)](#) introduce a hyperprior to capture uncertainty in EB estimation of prior hyperparameters in general hierarchical models. [Rousseau and Szabo \(2017\)](#) provide sufficient conditions for general consistency and posterior contraction rates of the EB posterior under parametric maximum marginal likelihood; in their setting, the results show that hierarchical and empirical Bayes posteriors obtain comparable posterior contraction rates. [Rizzelli et al. \(2024\)](#) analyze the asymptotic behavior of posteriors obtained after fitting such hyperparameters. [Buta and Doss \(2011\)](#) and [Doss and Linero \(2024\)](#) discussed the connection between empirical Bayes

and Bayesian sensitivity analysis. While the Bayesian literature on EB has focused almost exclusively on parametric models, Bayesian empirical Bayes provides a principled approach to nonparametric empirical Bayes, motivated from Bayesian reasoning.

Many objects in classical statistics obey probabilistic symmetries (see [Diaconis \(1988\)](#); see also Chapter 3 of [Lehmann and Casella, 2006](#)). The notion of *exchangeability*, for example, serves as the foundation for Bayesian theory ([Finetti, 1929](#); [Savage, 1954](#); [Bernardo and Smith, 1994](#)) and underlies much of practical Bayesian modeling ([Gelman et al., 1995](#)). Other applications of group symmetries include invariant testing—e.g., permutation-based testing methods ([Eden and Yates, 1933](#); [Fisher, 1935](#); [Pitman, 1937](#); [Pesarin, 2001](#); [Ernst, 2004](#); [Pesarin and Salmaso, 2010, 2012](#); [Good, 2006](#); [Anderson and Robinson, 2001](#); [Kennedy, 1995](#); [Hemerik and Goeman, 2018](#); [Ramdas et al., 2023](#)). Early advances for estimation and testing under general groups include [Lehmann and Stein \(1949\)](#) and [Hoeffding \(1952\)](#); the celebrated Hunt-Stein theorem states conditions under which a minimax invariant test exists in hypothesis testing ([Lehmann, 1959](#)). Broader treatments appear in [Eaton \(1989\)](#); [Wijsman \(1990\)](#); [Giri \(1996\)](#). In modern probabilistic modeling, the ergodic decomposition theorem provides a foundation for building invariant representations and modeling ([Orbánz and Roy, 2015](#)). For example, [Lloyd et al. \(2012\)](#) study exchangeable arrays by placing a Gaussian process prior on the underlying random function. We build on the general theory of probabilistic symmetries as developed in [Kallenberg \(2005\)](#) and [Orbánz and Roy \(2015\)](#). The theory characterizes general invariant distributions under group actions using ideas from ergodic theory. It allows us to extend empirical Bayes to many different kinds of structured data settings, creating a foundation for new applications of EB.

2 Bayesian Empirical Bayes

Consider a *structured dataset* $\mathbf{x} = (x_\omega)_{\omega \in \Omega}$, where each x_ω is indexed by an element in an index set Ω . For example, if $\Omega = \mathbb{N}$, then \mathbf{x} is an infinite sequence; if $\Omega = \mathbb{N}^2$, then \mathbf{x} is an infinite array. (After describing a model of infinite data, we will reduce it to one of finite data.)

We posit that the data \mathbf{x} are noisy measurements of a matching set of *structured latent variables* $\mathbf{z} = (z_\omega)_{\omega \in \Omega}$. In the likelihood, each x_ω is conditionally independent given its local latent z_ω ,

$$p(\mathbf{x} | \mathbf{z}) = \prod_{\omega \in \Omega} p(x_\omega | z_\omega). \quad (4)$$

We assume the form of the noise distribution $p(x_\omega | z_\omega)$ is known.

We place a prior distribution on the latent variables $\mathbf{z} \sim p(\mathbf{z})$. The joint distribution of \mathbf{z} and \mathbf{x} is now

$$p(\mathbf{z}, \mathbf{x}) = p(\mathbf{z}) \prod_{\omega \in \Omega} p(x_\omega | z_\omega). \quad (5)$$

Note, we do not assume independence in the prior.

Our goal is *simultaneous probabilistic inference* of all local latent variables across Ω . That is, we want to calculate the posterior $p(\mathbf{z}|\mathbf{x})$. From this posterior, we can calculate summary statistics, such as the posterior means $\mathbb{E}[\mathbf{z}|\mathbf{x}]$, or other quantities of interest, such as credible intervals, quantiles, posterior predictive distributions, or event probabilities. In short, we can denoise the data.

We now make the *empirical Bayes assumption*: there exists a prior $p^*(\mathbf{z})$ such that the true data-generating distribution of \mathbf{x} is expressed by marginalizing over \mathbf{z} .

Assumption 1 (Empirical Bayes). *There exists a prior $p^*(\mathbf{z})$ such that the true data-generating distribution can be written as*

$$p^*(\mathbf{x}) = \int_{\mathcal{Z}^\Omega} p^*(\mathbf{z}) \prod_{\omega \in \Omega} p(x_\omega | z_\omega) d\mathbf{z}.$$

Of course, we do not know this true prior ahead of time - we just assume it exists. We call this the empirical Bayes assumption because it links the Bayesian model to the true data-generating process.

2.1 Priors with Probabilistic Symmetries

How do we set the prior $p(\mathbf{z})$? We will use the idea of a *probabilistic symmetry*. A symmetry describes how we can relabel or transform the indices of structured random variables without changing their joint distribution.

Formally, let Φ denote a group of transformations acting bijectively on the index set Ω , where each element $\phi \in \Phi$ reindexes the coordinates of Ω . The action of ϕ on \mathbf{z} is the *index transformation*

$$(\phi(\mathbf{z}))_\omega = z_{\phi^{-1}(\omega)}, \quad \omega \in \Omega. \quad (6)$$

As examples, if $\Omega = \mathbb{N}$, then $\phi(\mathbf{z})$ reorders the elements of a sequence. If $\Omega = \mathbb{N}^2$, then $\phi(\mathbf{z})$ could permute rows and columns of a matrix. If $\Omega = \mathbb{R}^2$, then $\phi(\mathbf{z})$ could implement a spatial shift.

A distribution $p(\mathbf{z})$ is Φ -*invariant* if it does not change under these transformations. For example, an exchangeable sequence is invariant under permutations; a stationary process is invariant under spatial shifts.

Definition 1 (Φ -invariance). *A joint distribution $p(\mathbf{z})$ of structured variables $\mathbf{z} \in \mathcal{Z}^\Omega$ is Φ -invariant if*

$$\phi(\mathbf{z}) \stackrel{d}{=} \mathbf{z} \quad \text{for all } \phi \in \Phi, \quad (7)$$

where equality is in distribution for all finite-dimensional marginals.

A formal consequence of Φ -invariance is the *ergodic decomposition theorem*, which states that any Φ -invariant distribution can be expressed as a mixture of *ergodic distributions*.

Theorem 1 (Ergodic decomposition; [Varadarajan \(1963\)](#)). *Let Φ be a nice group acting on \mathcal{Z}^Ω . There exists a family of distributions*

$$\mathcal{E} := \{p(\mathbf{z}|g) : g \in \mathcal{G}\} \subseteq \mathcal{P}(\mathcal{Z}^\Omega) \quad (8)$$

such that any Φ -invariant distribution $p(\mathbf{z})$ admits the unique decomposition

$$p(\mathbf{z}) = \int_{\mathcal{G}} p(\mathbf{z}|g) d\mu(g), \quad (9)$$

*for some distribution μ on \mathcal{G} . The set \mathcal{E} is called the Φ -ergodic family and its index g is called the invariant variable.*¹

A “nice” group is a technical condition; see § A for a formal definition. The Φ -ergodic family is determined by the group Φ and forms the set of extreme points of the convex set of Φ -invariant distributions on \mathcal{Z}^Ω ([Kallenberg, 1997](#), Theorem 25.24). Once Φ is fixed, so too is the form of $p(\mathbf{z}|g)$.

The ergodic decomposition theorem generalizes de Finetti’s representation ([Finetti, 1929](#)) from exchangeable sequences to arbitrary group symmetries. Under exchangeability, the ergodic measures are precisely the i.i.d. product distributions.

The ergodic decomposition describes the structure of any Φ -invariant distribution. We now apply this idea to the true prior.

Assumption 2 (True Φ -invariant prior). *The true prior $p^*(\mathbf{z})$ is Φ -invariant.*

By Theorem 1, there exists an invariant variable $g \in \mathcal{G}$ with distribution $g \sim \mu^*$ such that $p^*(\mathbf{z})$ is a μ^* -mixture of the Φ -ergodic family,

$$p^*(\mathbf{z}) = \int_{\mathcal{G}} p(\mathbf{z}|g) d\mu^*(g). \quad (10)$$

Together, Assumptions 1 and 2 state that among all models of the form in Eq. 5, there exists a correctly specified version whose prior is Φ -invariant. In the Bayesian empirical Bayes model, the latent variables \mathbf{z} capture the structured, invariant part of the world, and the observations \mathbf{x} are noisy realizations through the shared likelihood $p(x_\omega | z_\omega)$.

An important consequence of Assumption 2 is that the data-generating distribution $p^*(\mathbf{x})$ inherits the same symmetry as the prior. To see this, we first note that applying any transformation $\phi \in \Phi$ to both \mathbf{x} and \mathbf{z} leaves the joint distribution unchanged,

$$p^*(\phi(\mathbf{x}), \phi(\mathbf{z})) = p^*(\mathbf{z}) \prod_{\omega \in \Omega} p(x_{\phi^{-1}(\omega)} | z_{\phi^{-1}(\omega)}) \quad (11)$$

$$= p^*(\mathbf{z}) \prod_{\omega \in \Omega} p(x_\omega | z_\omega) = p^*(\mathbf{x}, \mathbf{z}). \quad (12)$$

¹It is also known as the directing random measure ([Kallenberg, 2005](#)).

Then we marginalize out \mathbf{z} to give $p^*(\phi(\mathbf{x})) = p^*(\mathbf{x})$.

Alternatively, instead of assuming the true prior is invariant, we could assume that the marginal distribution of the data is invariant. Then, under mild regularity assumptions on the likelihood, the Φ -invariance of the population distribution $p^*(\mathbf{x})$ also implies the Φ -invariance of $p^*(\mathbf{z})$.

2.2 Examples of Φ -invariant priors

We present three examples of Φ -invariant priors, which we will use throughout this paper. In each, we specify the index set Ω , the symmetry group Φ , the form of the ergodic decomposition, and the corresponding invariant variable g .

Exchangeable sequences. Let $\Omega = \mathbb{N}$, so that $\mathbf{z} = (z_1, z_2, \dots)$ is a sequence of random variables. The symmetry group is $\Phi = \mathbb{S}$, the group of permutations of \mathbb{N} . The Φ -invariant distributions on $\mathcal{Z}^{\mathbb{N}}$ are the *exchangeable sequences*.

In this case, the ergodic decomposition recovers de Finetti's representation theorem (Finetti, 1929),

$$p(\mathbf{z}) = \int_{\mathcal{G}_{\text{perm}}} \prod_{\omega \in \Omega} g_{\text{perm}}(z_\omega) d\mu(g_{\text{perm}}). \quad (13)$$

The invariant variable g_{perm} is a random probability measure on \mathcal{Z} , and μ is a distribution over such random measures.

Exchangeable arrays. Let $\Omega = \mathbb{N}^2$, so that $\mathbf{z} = (z_{ij})_{i,j \in \mathbb{N}}$ is an array of random variables. The array is *separately exchangeable* if its distribution is invariant under the independent permutations of rows and columns. That is, the symmetry group is $\Phi = \mathbb{S}^2$, and

$$(z_{ij}) \stackrel{d}{=} (z_{\pi(i), \pi'(j)}) \quad \text{for all } (\pi, \pi') \in \Phi. \quad (14)$$

Under separate exchangeability, the Aldous–Hoover theorem provides the ergodic decomposition (Aldous, 1981, 2006).

Theorem 2 (Aldous–Hoover representation for separate exchangeability). *A random array $\mathbf{z} = (z_{ij})_{i,j \in \mathbb{N}}$ is separately exchangeable if and only if its distribution can be written as*

$$p(\mathbf{z}) = \int_{\mathcal{G}_{\text{sep}}} p(\mathbf{z} | g_{\text{sep}}) d\mu(g_{\text{sep}}). \quad (15)$$

The invariant variable is a random function

$$g_{\text{sep}} : [0, 1]^3 \rightarrow \mathcal{Z} \quad (16)$$

and the ergodic distribution $p(\mathbf{z} | g)$ is defined through uniform random variables

$$u_i, v_j, u_{ij} \stackrel{iid}{\sim} \text{unif}(0, 1) \quad z_{ij} = g_{\text{sep}}(u_i, v_j, u_{ij}) \quad \text{for all } i, j \in \mathbb{N}. \quad (17)$$

Through the shared row and column variables $(u_i)_{i \in \mathbb{N}}$ and $(v_j)_{j \in \mathbb{N}}$, the entries z_{ij} exhibit dependence within rows and within columns.

Variants of this representation capture other symmetry assumptions. If the array is *jointly exchangeable*—invariant when rows and columns are permuted together—then the same decomposition holds with

$$u_i, u_{ij} \stackrel{iid}{\sim} \text{Unif}(0, 1) \quad z_{ij} = g_{\text{joint}}(u_i, u_j, u_{ij}) \quad \text{for all } i, j \in \mathbb{N}.$$

In a binary array with joint exchangeability, i.e., a random graph, the Aldous–Hoover representation yields

$$z_{ij} = \mathbf{1}\{u_{ij} \leq g_{\text{graph}}(u_i, u_j)\},$$

for a random symmetric graphon $g_{\text{graph}} : [0, 1]^2 \rightarrow [0, 1]$. In § D.3, we discuss array exchangeability conditional on row- and column-specific covariates. [Orbanz and Roy \(2015\)](#) extends all these representations to k -arrays, where $\Omega = \mathbb{N}^k$.

Stationary processes. We now consider variables in time or space. Let $\Omega = \mathbb{R}^d$ (continuous space) or \mathbb{Z}^d (lattice), and $\mathcal{Z} = \mathbb{R}$. A distribution $p(\mathbf{z})$ on \mathcal{Z}^Ω is *stationary* if it is invariant under spatial shifts $\Phi_{\text{shift}} = \{\phi_h : \omega \mapsto \omega + h\}$ with $h \in \Omega$:

$$p(\phi_h^{-1}(A)) = p(A) \quad \text{for all measurable } A \subseteq \mathcal{Z}^\Omega, h \in \Omega.$$

Each such $p(\mathbf{z})$ is a *stationary probability measure*. Among these, a measure g_{erg} is called *ergodic* if it cannot be written as a nontrivial mixture of other stationary measures. Equivalently, it is ergodic if $g_{\text{erg}}(A) \in \{0, 1\}$ for every shift-invariant event A .

By the ergodic decomposition theorem ([Shields, 1996](#), Theorem I.4.10), any stationary measure can be written uniquely as a mixture of ergodic stationary measures,

$$p(\mathbf{z}) = \int_{\mathcal{G}} g_{\text{erg}}(\mathbf{z}) d\mu(g_{\text{erg}}), \tag{18}$$

where \mathcal{G} is the space of all ergodic stationary measures on \mathcal{Z}^Ω . Compared with exchangeable models, stationary processes impose a weaker symmetry: the discrete shift group grows only polynomially with system size, while the permutation group grows super-exponentially ([Lubotzky and Segal, 2003](#)). As a result, representation theorems for stationarity are less restrictive, but also less tractable.

2.3 The finite population model

We have defined our model in terms of the entire set Ω . But in practice we only observe finite data. We now specialize our population model to a finite domain.

Let $S_n \subseteq \Omega$ be a finite subset, with $S_1 \subseteq S_2 \subseteq \dots$ forming a nested sequence that exhausts Ω . We observe finite data $\mathbf{x}_n = (x_\omega)_{\omega \in S_n}$, each associated with a local latent variable z_ω . We write $\mathbf{z}_n = (z_\omega)_{\omega \in S_n}$. Intuitively, this means we observe a finite subset of the full population

\mathbf{x} at selected index locations, i.e. certain entries of an array or certain locations in time or space).

We first state the finite-data analog of the empirical Bayes assumption, that there exists a true prior that captures the population distribution.

Proposition 1 (Finite empirical Bayes model). *Under Assumption 1, the marginal distribution of the finite data \mathbf{x}_n can be written as*

$$p^*(\mathbf{x}_n) = \int_{\mathcal{Z}^{S_n}} p^*(\mathbf{z}_n) \prod_{\omega \in S_n} p(x_\omega | z_\omega) d\mathbf{z}_n,$$

for some prior $p^*(\mathbf{z}_n)$ on the latent variables indexed by S_n .

We next connect this finite prior to the group symmetry, and write its ergodic decomposition.

Proposition 2 (Finite Φ -invariant prior). *Suppose the population prior $p^*(\mathbf{z})$ is Φ -invariant as in Assumption 2. Then its marginal $p^*(\mathbf{z}_n)$ also admits an ergodic representation,*

$$p^*(\mathbf{z}_n) = \int_{\mathcal{G}} p(\mathbf{z}_n | g) d\mu^*(g),$$

where

$$p(\mathbf{z}_n | g) = \int_{\mathcal{Z}_{\Omega \setminus S_n}} p(\mathbf{z} | g) d\mathbf{z}_{\Omega \setminus S_n}$$

is the marginal of the ergodic distribution $p(\mathbf{z} | g)$ on S_n .

Consider a dataset \mathbf{x}_n and assume it was drawn from \mathbf{z}_n with a Φ -symmetric prior. As a consequence of Propositions 1 and 2, its generative process is a hierarchical model:

$$\begin{aligned} g &\sim \mu^* \\ \mathbf{z}_n &\sim p(\mathbf{z}_n | g) \\ x_\omega &\sim p(x | z_\omega) \quad \omega \in S_n. \end{aligned} \tag{19}$$

The latent variables are \mathbf{z}_n and g , and the observations are \mathbf{x}_n . The only unknown factor is the prior μ^* , because the likelihood $p(x | z)$ is fixed and the form of $p(\mathbf{z}_n | g)$ is known and determined by the probabilistic symmetry.

2.4 Bayesian empirical Bayes

We are given a dataset \mathbf{x}_n and assume a probabilistic symmetry on its prior $p(\mathbf{z}_n)$. Consequently, our data comes from the model in Eq. 19, with the form of the invariant variable g and ergodic distribution $p(\mathbf{z}_n | g)$ determined by the assumed symmetry. Our goal is to compute the posterior $p^*(\mathbf{z}_n | \mathbf{x}_n)$.

We first write the posterior as an integral

$$p^*(\mathbf{z}_n | \mathbf{x}_n) = \int_{\mathcal{G}} p(\mathbf{z}_n | g, \mathbf{x}_n) p^*(g | \mathbf{x}_n) dg. \tag{20}$$

Note the conditional distribution $p(\mathbf{z}_n | \mathbf{g}, \mathbf{x}_n)$ is proportional to the product of the likelihood $p(\mathbf{x}_n | \mathbf{z}_n)$ and the ergodic distribution $p(\mathbf{z}_n | \mathbf{g})$:

$$p(\mathbf{z}_n | \mathbf{g}, \mathbf{x}_n) \propto p(\mathbf{x}_n | \mathbf{z}_n) p(\mathbf{z}_n | \mathbf{g}), \quad (21)$$

where both these terms are known. The only unknown component in Eq. 20 is $p^*(\mathbf{g} | \mathbf{x}_n)$, which depends on the unknown μ^* .

We next approximate $p^*(\mathbf{g} | \mathbf{x}_n)$ by a point estimate $\hat{\mathbf{g}}$ at its value that maximizes the marginal likelihood of the data,

$$\hat{\mathbf{g}} \in \arg \max_{\mathbf{g} \in \mathcal{G}} \log \int_{\mathcal{Z}^{S_n}} p(\mathbf{z}_n | \mathbf{g}) \prod_{\omega \in S_n} p(x_\omega | z_\omega) d\mathbf{z}_n. \quad (22)$$

The form of $\mathbf{g} \in \mathcal{G}$ depends on the chosen symmetry. For example, in exchangeable data, \mathbf{g} is a prior on \mathbf{z} and \mathcal{G} is the space of such priors. In separately-exchangeable array data, \mathbf{g} are the functions described in Eq. 16; we will parameterize them with neural networks to capture a large space \mathcal{G} .

This approximation is motivated by both asymptotic and computational considerations. The observed dataset \mathbf{x}_n is generated from a single draw \mathbf{g}^* . So asymptotically, we expect the ideal posterior $p^*(\mathbf{g} | \mathbf{x}_n)$ to concentrate at \mathbf{g}^* as $n \rightarrow \infty$. In particular, by Theorem 1, the law $p(\mathbf{z} | \mathbf{g})$ is Φ -ergodic and hence identifiable (see, e.g., (Kallenberg, 1997, Lemma 27.1) and (Lindenstrauss, 2001, Theorem 1.2)). Under a characteristic likelihood, such as the normal model with known variance, distinct priors $p(\mathbf{z} | \mathbf{g})$ induce distinct marginals $p(\mathbf{x} | \mathbf{g})$, so \mathbf{g} is identifiable from $p(\mathbf{x} | \mathbf{g})$. Posterior concentration then follows from Doob's theorem (Ghosal and van der Vaart, 2017, Ch. 6). Computationally, although the marginal likelihood in Eq. 22 may be intractable, we can use variational inference to approximate it (Blei et al., 2017).

Finally, we substitute the point-estimate approximation of the prior into the posterior of Eq. 20. This gives the approximation

$$\hat{p}(\mathbf{z}_n | \mathbf{x}_n) := p(\mathbf{z}_n | \hat{\mathbf{g}}, \mathbf{x}_n). \quad (23)$$

We estimate $p(\mathbf{z}_n | \mathbf{x}_n, \hat{\mathbf{g}})$, given in Eq. 21, by exact or approximate methods. For example, we can use variational inference or MCMC.

Our procedure is called *Bayesian empirical Bayes (BEB)*. We are given data \mathbf{x}_n and assume a symmetry group Φ for the latent variables \mathbf{z}_n . We use the ergodic representation theorem to form the expanded hierarchical model (Eq. 19), which includes the invariant variable \mathbf{g} and the corresponding ergodic family $p(\mathbf{z} | \mathbf{g})$. We parameterize \mathbf{g} and estimate it from data via maximum marginal likelihood (Eq. 22) or a suitable surrogate. Finally, we plug the estimate $\hat{\mathbf{g}}$ into the conditional posterior (Eq. 23). Algorithm 1 presents this recipe.

3 New Models for Empirical Bayes

We now use BEB to design new methods for empirical Bayes inference. In our first example, we use BEB to recover the classical empirical Bayes \mathbf{g} -modeling for the normal means

Algorithm 1: Bayesian Empirical Bayes

Input: Data \mathbf{x}_n , likelihood model $p(\mathbf{x}_n | \mathbf{z}_n)$, group Φ .

Steps:

1. Derive the ergodic decomposition $p(\mathbf{z}_n | \mathbf{g})$ from Φ .
2. Estimate $\hat{\mathbf{g}}$ by maximizing the marginal likelihood or a surrogate:

$$\hat{\mathbf{g}} \in \arg \max_{\mathbf{g} \in \mathcal{G}} \log p(\mathbf{x}_n; \mathbf{g}).$$

3. Approximate the posterior of the latent \mathbf{z}_n :

$$\hat{p}(\mathbf{z}_n | \mathbf{x}_n) \propto p(\mathbf{x}_n | \mathbf{z}_n) p(\mathbf{z}_n | \hat{\mathbf{g}}).$$

Output: Approximate posterior $\hat{p}(\mathbf{z}_n | \mathbf{x}_n)$

model (§ 3.1). This recovers classical EB methods (Efron, 2015a; Soloff et al., 2025). We then extend EB to additional probabilistic symmetries: separate/joint exchangeability in arrays (§ 3.2), stationarity in spatial data (§ 3.3), and relative exchangeability conditional on covariates (§ D.3). In each case, we follow the recipe of Algorithm 1. We start with a dataset, a symmetry group, and a likelihood. We then design an empirical Bayes model–tailored to the symmetry–and approximate the posterior of the latent structured variables.

3.1 Classical Example Revisited: Normal Means Model

Let $\Omega = \mathbb{N}$ and $\mathcal{X} = \mathbb{R}^d$. The observed variables $\mathbf{x} \in \mathcal{X}^\Omega$ are generated from the heteroskedastic normal means model

$$\mathbf{z} \sim p^*(\mathbf{z}), \quad x_i \sim \mathcal{N}(z_i, \Sigma_i), \quad (24)$$

where $\Sigma_i \in \mathbb{R}^{d \times d}$ is known.

We assume the true prior $p^*(\mathbf{z})$ is exchangeable. By de Finetti’s theorem, we can write Eq. 24 as the following generative process:

$$\mathbf{g}_{\text{perm}} \sim \mu^*, \quad z_i \stackrel{iid}{\sim} \mathbf{g}_{\text{perm}}, \quad x_i \sim \mathcal{N}(z_i, \Sigma_i). \quad (25)$$

Here \mathbf{g}_{perm} is a random prior over \mathbf{z} . In short, de Finetti’s representation specializes Theorem 1 to sequences, with $\prod_{i=1}^{\infty} \mathbf{g}_{\text{perm}}(z_i)$ the ergodic distribution.

Under the expanded model, the posterior $p^*(\mathbf{z}_n | \mathbf{x}_n)$ has the form

$$p^*(\mathbf{z}_n | \mathbf{x}_n) = \int_{\mathcal{G}} \prod_{i=1}^n p(z_i | \mathbf{g}_{\text{perm}}, x_i) p^*(\mathbf{g}_{\text{perm}} | \mathbf{x}_n) d\mathbf{g}_{\text{perm}}. \quad (26)$$

In Bayesian EB, we approximate $p^*(\mathbf{g}_{\text{perm}} | \mathbf{x}_n)$ with its maximum marginal likelihood

estimator (MMLE),

$$\hat{g}_{\text{perm}} \in \arg \max_{g_{\text{perm}} \in \mathcal{P}(\mathbb{R}^d)} \log \int_{\mathcal{X}^n} \prod_{i=1}^n \left(p(x_i | z_i) g_{\text{perm}}(z_i) \right) dz_n. \quad (27)$$

If we restrict g_{perm} to a parametric family, then this recovers parametric empirical Bayes estimation, or type-II maximum likelihood. If we consider all possible priors, then it recovers the nonparametric maximum likelihood estimation (NPMLE) approach.

With \hat{g}_{perm} in hand, we approximate the target posterior from Eq. 26,

$$p^*(z_n | x_n) \approx \prod_{i=1}^n p(z_i | x_i, \hat{g}_{\text{perm}}),$$

where each posterior is

$$p(z_i | x_i, \hat{g}_{\text{perm}}) \propto p(x_i | z_i) \hat{g}_{\text{perm}}(z_i).$$

NPMLE and the normal means model have been thoroughly studied in numerous works (Kiefer and Wolfowitz, 1956; James and Stein, 1960; Jiang and Zhang, 2009; Brown and Greenshtein, 2009; Jiang and Zhang, 2010; Xie et al., 2012; Efron, 2012, 2015a; Tan, 2016; Brown et al., 2018; Jiang, 2020; Chen, 2022; Soloff et al., 2025).

If the likelihood is non-Gaussian, the same reasoning yields other nonparametric EB g-modeling procedures. For example, with exponential data $x_i | z_i \sim \text{Exp}(z_i)$, this approach recovers g-modeling for the exponential sequence model (Robbins, 1980). As another example, when x_i is a sample variance and z_i the true variance, we obtain the χ^2 sequence model $x_i | z_i \sim (z_i/k) \chi_k^2$ (for known k). The exchangeability assumption on z_1, \dots, z_n recovers the g-modeling setting studied in Ignatiadis and Sen (2025b).

Denoising an MNIST digit. We now introduce a running example to illustrate the performance of Bayesian EB methods. The dataset is an image of "5" from the MNIST dataset of handwritten digits (LeCun et al., 2002). The 28×28 image is corrupted by i.i.d. Gaussian noise with variance equal to the empirical pixel variance of the clean image

$$x_{\omega} \sim \mathcal{N}(z_{\omega}^*, \sigma_0^2), \quad \omega \in [28]^2.$$

The goal is to recover the clean image $z_{n,n}^*$ from the observed noisy image $x_{n,n}$. The maximum likelihood estimator is the simply the noisy image which has a MSE of 10.291. The exchangeable sequence approach treats the problem as a simple normal means problem with known variance σ_0^2 and applies the NPMLE procedure. The resulting MSE is 3.61—a substantial reduction from the error of the observed image. The first three panels in Figure 1 display the results.

3.2 Bayesian empirical Bayes for matrix recovery

Let $\Omega = \mathbb{N}^2$ and $\mathcal{X} = \mathbb{R}$. We observe a noisy array $\mathbf{x}_{n,p} = (x_{ij})_{i \in [n], j \in [p]}$ with latent signal $\mathbf{z}_{n,p} = (z_{ij})_{i \in [n], j \in [p]}$ generated by

$$x_{ij} \sim \mathcal{N}(z_{ij}, \tau_{ij}^{-1}), \quad \tau_{ij} > 0.$$

Our goal is to estimate $\mathbf{z}_{n,p}$ from $\mathbf{x}_{n,p}$. We will use BEB to fit a structured prior that captures dependencies among entries.

We assume \mathbf{z} is *separately exchangeable*: its distribution is invariant to independent permutations of rows and columns. Recall by the Aldous–Hoover theorem (Theorem 2), we can write the conditional distribution $p(\mathbf{z}_n | \mathbf{g}_{\text{sep}})$ as

$$u_i, v_j, u_{ij} \stackrel{iid}{\sim} \text{unif}[0, 1], \quad z_{ij} = \mathbf{g}_{\text{sep}}(u_i, v_j, u_{ij}), \quad (28)$$

where the invariant variable is a function $\mathbf{g}_{\text{sep}} : [0, 1]^3 \rightarrow \mathbb{R}$. This conditional representation fully characterizes the finite-dimensional marginals of the ergodic distribution $p(\mathbf{z} | \mathbf{g}_{\text{sep}})$, in the context of Theorem 1.

The corresponding Bayesian empirical Bayes model is

$$\begin{aligned} \mathbf{g}_{\text{sep}} &\sim \mu^*, \\ u_i, v_j, u_{ij} &\stackrel{iid}{\sim} \text{unif}[0, 1], \quad i \in [n], j \in [n] \\ z_{ij} &= \mathbf{g}_{\text{sep}}(u_i, v_j, u_{ij}), \\ x_{ij} &\sim \mathcal{N}(z_{ij}, \tau_{ij}^{-1}). \end{aligned} \quad (29)$$

We parameterize \mathbf{g}_{sep} by a neural network $\mathbf{g}_{\text{sep}, \theta} \in \mathcal{G}_{\text{NN}}$, a two-layer ReLU feed-forward network mapping $[0, 1]^3$ to \mathbb{R} . We estimate θ by marginal maximum likelihood, now writing the conditional distribution of x_{ij} directly in terms of $\mathbf{u}_n, \mathbf{v}_p, \mathbf{u}_{n,p}$,

$$\hat{\theta} \in \arg \max_{\theta \in \Theta} \log \int \int \int \prod_{i=1}^n \prod_{j=1}^p p(x_{ij} | \mathbf{g}_{\text{sep}, \theta}(u_i, v_j, u_{ij})) d\mathbf{u}_n d\mathbf{v}_p d\mathbf{u}_{n,p}. \quad (30)$$

Exact evaluation of Eq. 30 is intractable because the integral is high-dimensional. We approximate it by maximizing an evidence lower bound (ELBO) under a structured variational family. The estimate $\hat{\mathbf{g}}_{\text{sep}, \theta}$ is the variational MMLE. See § D for details.

Given $\hat{\mathbf{g}}_{\text{sep}, \theta}$, we approximate the empirical Bayes posterior for $\mathbf{z}_{n,p}$ with samples, through the posterior of $\mathbf{u}_n, \mathbf{v}_p, \mathbf{u}_{n,p}$. For each sample s ,

$$\begin{aligned} \mathbf{u}_n^{(s)}, \mathbf{v}_p^{(s)}, \mathbf{u}_{n,p}^{(s)} &\sim p(\mathbf{u}_n, \mathbf{v}_p, \mathbf{u}_{n,p} | \mathbf{x}_{n,p}, \hat{\mathbf{g}}_{\text{sep}}) \\ z_{ij}^{(s)} &= \hat{\mathbf{g}}_{\text{sep}}(u_i^{(s)}, v_j^{(s)}, u_{ij}^{(s)}). \end{aligned}$$

The conditional posterior of the auxiliary latent variables is

$$p(\mathbf{u}_n, \mathbf{v}_p, \mathbf{u}_{n,p} | \mathbf{x}_{n,p}, \hat{\mathbf{g}}_{\text{sep}}) \propto \prod_{i=1}^n \prod_{j=1}^p \mathcal{N}\left(x_{ij}; \hat{\mathbf{g}}_{\text{sep}}(u_i, v_j, u_{ij}), \tau_{ij}^{-1}\right), \quad (31)$$

which we sample from using the No-U-Turn Sampler (NUTS; [Hoffman and Gelman, 2014](#)) or a variational approximation.

Related symmetries. If the array is *jointly exchangeable* then it is invariant when rows and columns are permuted together. In this case, Eq. 28 simplifies to

$$u_i, u_{ij} \stackrel{iid}{\sim} \text{unif}[0, 1], \quad z_{ij} = g_{\text{joint}}(u_i, u_j, u_{ij}),$$

with $g_{\text{joint}} : [0, 1]^3 \rightarrow \mathbb{R}$. We follow nearly the same procedure.

If the array is *relatively exchangeable* conditioned on row covariates $\mathbf{y}_n = (y_i)_{i=1}^n$ with $y_i \in \mathcal{Y}$ and column covariates $\mathbf{a}_p = (a_j)_{j=1}^p$ with $a_j \in \mathcal{A}$, then Eq. 28 expands to

$$u_i, v_j, u_{ij} \stackrel{iid}{\sim} \text{unif}[0, 1], \quad z_{ij} = g_{\text{rel}}(y_i, a_j, u_i, v_j, u_{ij}),$$

with $g_{\text{rel}} : \mathcal{Y} \times \mathcal{A} \times [0, 1]^3 \rightarrow \mathbb{R}$. This yields the covariate-assisted Bayesian empirical Bayes procedure developed in § D.3.

If the array is *fully exchangeable* then it is invariant to shuffling all of its cells. This case reduces to the algorithms of § 3.1, where $z_{ij} \stackrel{iid}{\sim} g_{\text{perm}}$ for a random measure g_{perm} .

Denoising an MNIST digit (continued). We revisit the example of denoising an MNIST "5" from Figure 1. The image is treated as a noisy matrix and we apply the proposed empirical Bayes matrix recovery (EBMR) methods under separate and joint exchangeability. We report $100 \times \text{MSE}$ between the posterior means $\hat{\mathbf{z}}_{n,n}$ and the true pixel value $\mathbf{z}_{n,n}^*$. The fourth and fifth panels in Figure 1 show the results. EBMR with a jointly exchangeable prior (EBMR–Joint) achieves the lowest error, followed by EBMR with a separately exchangeable prior (EBMR–Sep), then EBMR with a fully exchangeable prior (NPMLE). This ordering aligns with the symmetry hierarchy full \Rightarrow separate \Rightarrow joint: weaker (less restrictive) symmetry assumptions enlarge the class of admissible priors and increase flexibility. On the other hand, weaker symmetry assumptions also increase the sample and computational complexity for estimating g . This creates a trade-off. In our setting, joint exchangeability offers a sweet spot between expressiveness and efficiency.

3.3 Bayesian empirical Bayes for spatial regression

Let $\Omega = \mathbb{R}^d$ and $\mathcal{X} = \mathbb{R}$. We observe $\mathbf{x}_n = \{x_\omega : \omega \in S_n\}$ at sites $S_n \subset \Omega$. Each site has covariates $a_\omega = (a_{\omega,1}, \dots, a_{\omega,p}) \in \mathbb{R}^p$. The *spatial regression model* is

$$x_\omega = \beta^\top a_\omega + z_\omega + \varepsilon_\omega, \quad \varepsilon_\omega \sim \mathcal{N}(0, \tau_\omega^{-1}), \quad \tau_\omega > 0, \quad (32)$$

where $\beta \in \mathbb{R}^p$ are regression coefficients and $\mathbf{z} = (z_\omega)_{\omega \in \Omega}$ is a latent process that captures spatial dependence. We place a flat prior $\pi(\beta) \propto 1$, so the estimator of β coincides with weighted least squares. The resulting model along with Eq. 32 coincide with the standard model in Bayesian spatial regression (Handcock and Stein, 1993; Stein, 1999; Oliveira et al., 1997; Berger et al., 2001; Banerjee et al., 2008, 2015; Li et al., 2024).

We assume \mathbf{z} is *stationary*: its distribution is invariant under translations $\phi_h : \omega \mapsto \omega + h$. Following the ergodic decomposition in Eq. 18, any stationary process can be written as a mixture of *ergodic stationary measures*,

$$\mathbf{g} \sim \mu^*, \quad \mathbf{z} | \mathbf{g} \sim \mathbf{g}, \quad (33)$$

where \mathbf{g} is a stationary probability measure on \mathbb{R}^Ω . Following the BEB method, our goal is to estimate the invariant variable \mathbf{g} from data.

Defining stationary measures with Gaussian processes. The space of stationary measures is complex and so, in practice, we restrict the ergodic family \mathcal{G} to stationary ergodic Gaussian processes. A Gaussian process $\text{GP}(0, k)$ is stationary if its covariance function depends only on the displacement $k(\omega, \omega') = f(\omega - \omega') := k(\Delta)$. Each stationary covariance function k with an atomless spectral density (as described below) defines an ergodic stationary Gaussian measure on \mathbb{R}^Ω (Maruyama, 1949). So we can write

$$k \sim \mu(k), \quad \mathbf{z} | k \sim \text{GP}(0, k), \quad (34)$$

where $\mu(k)$ is a distribution over stationary kernels.

How can we characterize the stationary covariance functions? *Bochner's theorem* (Bochner, 2005) states that k is stationary and positive definite if and only if it can be written as

$$k(\Delta) = \int_{\mathbb{R}^d} e^{2\pi i s^\top \Delta} \psi(s) ds, \quad (35)$$

for some nonnegative integrable function ψ . The function $\psi : \mathbb{R}^d \rightarrow [0, \infty)$ is called the *spectral density*. It describes how the variance of the process is distributed across spatial frequencies. The associated spectral measure is *atomless* if it assigns zero mass to every singleton, i.e., $\Psi(s) = 0$ for all $s \in \mathbb{R}^d$ (in particular, if Ψ has density ψ , it is atomless). Bochner's theorem gives a one-to-one correspondence between stationary Gaussian measures and their spectral densities. We therefore identify each ergodic stationary measure \mathbf{g} with its spectral density ψ :

$$\psi \sim \mu^*, \quad \mathbf{z} | \psi \sim \text{GP}(0, k_\psi), \quad (36)$$

where k_ψ is the kernel defined by (35). The empirical Bayes task is to estimate ψ from the marginal distribution of the observed data.

Bayesian empirical Bayes for spatial regression. We have defined the invariant variable g as the spectral density of a stationary kernel for a Gaussian process. With this definition, the BEB model is

$$\mathbf{z} \sim \text{GP}(0, k_\psi), \quad \beta \sim \pi(\beta) \propto 1, \quad x_\omega \sim \mathcal{N}(\beta^\top a_\omega + z_\omega, \tau_\omega^{-1}). \quad (37)$$

We estimate the invariant variable ψ by maximizing the marginal likelihood,

$$\hat{\psi} \in \arg \max_{\psi \in \mathcal{G}} \log \int \left[\prod_{\omega \in S_n} p(x_\omega | z_\omega, \beta) \right] p(\mathbf{z}_n | \psi) \pi(\beta) d\beta d\mathbf{z}_n. \quad (38)$$

This is the empirical Bayes estimate of the stationary measure. Given $\hat{\psi}$, we compute the posterior $p(\beta, \mathbf{z}_n | \mathbf{x}_n, \hat{\psi})$, which is Gaussian with known mean and covariance. The BEB method thus fits the spectral density ψ , or equivalently the kernel k_ψ , that best explains the marginal distribution of the observed data.

In practice, we model ψ as a mixture of Gaussians, and fit it by maximum marginal likelihood. The details of this procedure, as well as how we perform simultaneous posterior inference, are given in § E.

In the spatial regression example, we model the spectral density of the Gaussian-process kernel as a mixture of Gaussian distributions. Under this model, the empirical Bayes procedure reduces to selecting the GP kernel parameters by maximum likelihood (Rasmussen and Williams, 2006). This approach is a common practice in the GP literature. It comes with strong theoretical guarantees and retains the conjugacy of the GP posterior (Loh and Lam, 2000; Bachoc, 2014; Szabó et al., 2015; Xu and Stein, 2017). What we see here is that this approach can be interpreted as an instance of Bayesian empirical Bayes.

Denoising an MNIST digit (continued). The image of a handwritten digit does not change its meaning if we shift the image, so stationarity is a reasonable assumption. We fit EB spatial regression with a constant covariate ($a_\omega \equiv 1$) and a $K = 10$ Gaussian-mixture spectral density, using the inference and sampling steps outlined in § E. The rightmost panel of Figure 1 shows that EB spatial regression denoises better than NPMLE but not as well as EBMR-sep or EBMR-joint. Nonetheless, all EB methods substantially improve over the MLE. Moreover, all BEB methods that use symmetries beyond exchangeability improve over the NPMLE.

4 Simulation Studies

We evaluate the new Bayesian empirical Bayes methods using synthetic data.

- In § 4.1, we assess empirical Bayes matrix recovery (EBMR; § 3.2) across 60 settings by varying sample size, noise level, and the data-generating mechanism; we implement EBMR with a separately exchangeable prior (EBMR-Sep) and compare against NPMLE and empirical Bayes matrix factorization (EBMF; Wang and Stephens (2021)).

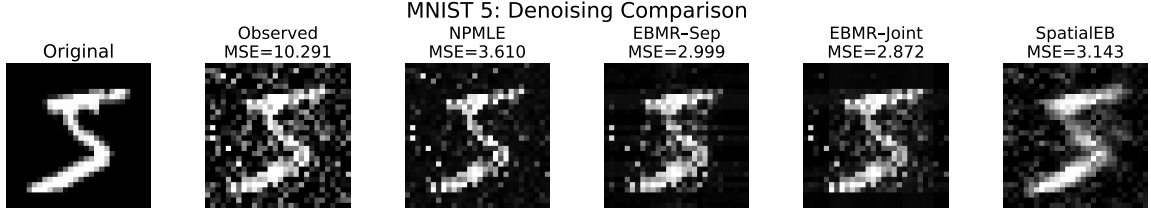


Figure 1: Denoising a noisy MNIST “5” with Bayesian empirical Bayes methods. Top: original (left), noisy (middle), and NPMLE (right). Bottom: EBMR–sep (left), EBMR–joint (middle), and EB spatial regression (right). Errors are $100 \times \text{MSE}$ of posterior means; EBMR with a jointly exchangeable prior performs best, followed by EBMR with a separately exchangeable prior and EB spatial regression, then NPMLE.

- In § 4.2, we evaluate the covariate-assisted empirical Bayes (CAEB; § D.3) method for denoising matrices with row- and column-specific covariates and compare it to EBMR–Sep, EBMF, and NPMLE.
- In § 4.3, we apply empirical Bayes spatial regression (spatial EB; § 3.3) to synthetic time-series data. We show that the MSE of EB spatial regression vanishes with increasing sample size, whereas the NPMLE plateaus at a constant risk.

In each study, we generate observations \mathbf{x}_{S_n} on a finite domain S_n (e.g. $S_n = [n]$) from a known data-generating process with latent truth $\mathbf{z}_{S_n}^*$. We report the relative MSE to assess how well the BEB posterior mean $\hat{\mathbf{z}}_{S_n}$ recovers the true latent values $\mathbf{z}_{S_n}^*$. The relative MSE measures the MSE of the estimator as a percentage of the MSE of the MLE (out of 100):

$$\text{R-MSE} = \frac{1}{|S_n|} \sum_{\omega \in S_n} (\hat{z}_\omega - z_\omega^*)^2 \times 100 \times \tau,$$

where τ is the precision of the noise distribution.

A better method achieves lower R-MSE.

4.1 Empirical Bayes Matrix Recovery

In our first study, we simulate observations from the normal means model $x_{ij} \sim \mathcal{N}(z_{ij}^*, \tau^{-1})$ with known precision $\tau > 0$. The true matrix $\mathbf{z}_{n,p}^*$ is a single draw from the Aldous–Hoover representation with a pre-specified function T_0 , that is

$$u_i, v_j, u_{ij} \stackrel{iid}{\sim} \text{unif}[0, 1], \quad z_{ij}^* = T_0(u_i, v_j, u_{ij}).$$

We consider five choices of T_0 , and vary the precisions $\tau \in \{0.25, 1, 2, 4\}$ and the sample sizes $(n, p) \in \{(20, 20), (20, 50), (50, 50)\}$. The different T_0 are as follows:

- **Linear:** $T_0(U, V, W) = U + V + W$;
- **Sine–log:** $T_0(U, V, W) = \sin(\pi UV) + \log(1 + W)$;

- **Sine–cos:** $T_0(U, V, W) = \frac{\sin(\pi U) \cos(\pi V)}{1 + W^2};$
- **Tanh:** $T_0(U, V, W) = \tanh(U + V + W);$
- **Reciprocal:** $T_0(U, V, W) = \frac{1}{1 + |U + V + W|}.$

We examine all combinations of (τ, n, p, T_0) for a total of 60 settings. For each setting, we run the experiment 10 times to calculate the R-MSE. We compare EBMR with a separately exchangeable prior (EBMR–Sep, Algorithm 2) against three benchmarks:

- **Benchmark 1: MLE.** The MLE is $\hat{z}_\omega = x_\omega$; by construction its R-MSE equals 100.
- **Benchmark 2: NPMLE.** NPMLE-based methods are state of the art for normal-means denoising problems (Jiang and Zhang, 2009; Koenker and Mizera, 2014; Soloff et al., 2025). In the context of matrix recovery, it is equivalent to EBMR with a fully exchangeable prior, $z_\omega \stackrel{iid}{\sim} g$. We estimate g via the nonparametric MLE using sequential quadratic programming (Kim et al., 2020), implemented with `ebnm` in R.
- **Benchmark 3: Empirical Bayes Matrix Factorization (EBMF).** EBMF (Wang and Stephens, 2021) models the latent matrix as low rank with exchangeable loadings and factors,

$$\mathbf{z}_{n,p} = \sum_{k=1}^C \ell_k f_k^\top, \quad \ell_k \in \mathbb{R}^n, f_k \in \mathbb{R}^p,$$

with $\{\ell_k\}_{k=1}^C \stackrel{iid}{\sim}$ from an unknown prior g_ℓ and $\{f_k\}_{k=1}^C \stackrel{iid}{\sim}$ from an unknown prior g_f . The priors (g_ℓ, g_f) are fit by variational empirical Bayes under the normal-means likelihood for $\mathbf{x}_{n,p}$, and we use the posterior mean of $\mathbf{z}_{n,p}$ as the estimator. Unless noted otherwise, we set $C = 10$ and implement the method using the `flashier` package in R.

To implement Algorithm 2, we set $K = 10$ and parameterize $g_{\text{sep}} : [0, 1]^3 \mapsto \mathbb{R}$ as a fully connected feed-forward MLP with two hidden layers, ReLU activations, and 5 units per layer. We choose a simple network configuration because the sample sizes are small.

Table 1 shows the results that EBMR–Sep outperforms NPMLE and EBMF in 55 out of the 60 settings. When T_0 introduces nonlinear dependencies across rows and columns (e.g., the sine–log function), the error reduction of EBMR–Sep relative to NPMLE and EBMF is substantial. The few cases where EBMF outperforms EBMR–Sep appear for small sample sizes—e.g., $(n, p) = (20, 20)$ —in settings where the latent factors (u_i, v_j) interact via an approximate low-rank structure (as with the sine–cos function).

4.2 Covariate-Assisted Empirical Bayes

We evaluate the posterior-mean estimator of covariate-assisted empirical Bayes (CAEB; § D.3) for matrix recovery with side information. Data are generated according to

$$z_{ij}^* = T_0(y_i, a_j, u_i, v_j, w_{ij}), \quad x_{ij} \sim \mathcal{N}(z_{ij}^*, 1),$$

Table 1: *EBMR-Sep attains the lowest R-MSE in 55 of 60 settings.* Matrix-recovery performance for NPMLE, EBMR with a separately exchangeable prior (Sep), and EBMF across simulated settings. Reported values are the median relative MSE (R-MSE), defined as each method’s MSE as a percentage of the MSE of the MLE. The lowest R-MSE in each setting is shown in **bold**.

n	p	τ	Linear			Sine-log			Sine-cos			Tanh			Reciprocal		
			NPMLE	Sep	EBMF	NPMLE	Sep	EBMF	NPMLE	Sep	EBMF	NPMLE	Sep	EBMF	NPMLE	Sep	EBMF
20	20	0.1	3.23	3.31	9.16	2.09	1.90	9.24	2.85	2.33	2.14	1.08	0.60	7.57	0.88	0.53	1.84
20	20	0.25	7.28	6.45	10.15	3.83	3.50	9.95	5.64	4.83	5.36	0.96	0.58	8.63	0.75	0.43	4.61
20	20	1	23.35	15.99	18.56	13.47	11.93	14.83	18.74	10.01	9.24	2.87	2.22	9.92	1.83	1.56	9.91
20	20	4	53.24	34.80	43.95	36.01	26.62	31.50	48.74	14.57	13.19	8.93	7.16	13.07	4.65	4.27	10.72
20	50	0.1	2.88	2.76	8.26	2.00	1.73	10.38	2.49	2.27	2.06	0.65	0.39	7.75	0.61	0.49	1.75
20	50	0.25	6.38	5.11	9.79	4.17	3.55	8.27	5.31	3.54	5.14	0.87	0.47	5.68	0.70	0.30	4.38
20	50	1	20.13	12.47	22.78	14.11	9.04	18.03	17.94	6.22	20.55	2.29	1.42	8.05	1.73	0.92	7.35
20	50	4	49.97	29.56	69.45	38.82	22.01	49.92	44.95	8.67	37.59	5.55	4.77	10.64	3.15	3.00	9.00
50	50	0.1	2.69	2.24	4.73	1.69	1.45	4.00	1.88	1.22	1.84	0.37	0.27	3.65	0.25	0.20	1.95
50	50	0.25	6.21	4.30	6.00	3.86	3.06	5.13	4.49	2.12	4.61	0.65	0.61	4.05	0.38	0.32	4.83
50	50	1	20.65	10.76	12.23	13.54	7.49	8.63	15.73	2.76	4.48	2.27	1.98	4.84	1.24	1.01	4.32
50	50	4	50.99	28.45	37.36	38.32	19.66	23.11	42.34	4.85	6.28	8.07	5.77	7.77	4.03	3.32	5.09

where $y_i \in \mathbb{R}^3$ and $a_j \in \mathbb{R}^4$ are global row- and column-specific covariates, u_i and v_j are latent factors, and w_{ij} is an additional stochastic input.

We simulate y_i as iid draws from a standard t -distribution with 5 degrees of freedom and a_j from a beta distribution with $a = 2$ and $b = 5$. We consider three choices of T_0 :

- **Linear:** $T_0(y, a, u, v, w) = \sum_{k=1}^3 y[k] + \sum_{k=1}^4 a[k] + uv + w$
- **Nonlinear:** $T_0(y, a, u, v, w) = \sum_{k=1}^3 y[k] + \sum_{k=1}^4 a[k] + \sin(\pi u) \cos(\pi v) + 0.5w^2$
- **Logistic:** $T_0(y, a, u, v, w) = \sum_{k=1}^3 y[k] + \sum_{k=1}^4 a[k] + \text{sigmoid}(u + v) + w$

where $y[k]$ and $a[k]$ denote the k th coordinates of $y \in \mathbb{R}^3$ and $a \in \mathbb{R}^4$.

Implementation of covariate-assisted EB. We compare CAEB, EBMR–Sep, NPMLE, EBMF, and MLE. To implement CAEB, we parameterize $g_{\text{rel}} : \mathbb{R}^7 \times [0, 1]^3 \mapsto \mathbb{R}$ as a two-layer ReLU neural network with 10 hidden units per layer. We perform the stochastic gradient step using Adam and use NUTS with a target acceptance probability of 0.8 to sample from the posterior.

Table 2 reports the median R-MSE of the competing methods. CAEB consistently outperforms the NPMLE. In some cases, covariate-assisted EB achieves 10%–20% of the R-MSE of the NPMLE method. Thus, for simulated matrix data with covariates, covariate-assisted EB provides a markedly better denoising procedure than NPMLE.

Table 2 also shows that Bayesian EB methods achieve lower R-MSE than NPMLE. For smaller matrices $(n, p) \in \{(20, 20), (20, 50)\}$, EBMR–Sep beats CAEB. The reason is that estimating the 10-dimensional map g_{rel} requires more data than the 3-dimensional g_{sep} . Once $n, p \geq 50$, CAEB overtakes EBMR–Sep. At $n = p = 100$, the sample size suffices to fit the 10-dimensional network for g_{rel} , and the benefit of covariates becomes evident. Figure 2

n	p	Linear				Logistic				Nonlinear			
		CAEB	SEP	NPMLE	EBMF	CAEB	SEP	NPMLE	EBMF	CAEB	SEP	NPMLE	EBMF
20	20	50.63	18.79	77.19	24.66	44.45	18.63	82.69	20.83	42.76	17.55	81.10	20.88
20	50	29.25	15.69	75.59	28.82	27.23	13.93	75.71	27.20	28.37	14.74	79.83	43.26
20	100	20.21	12.92	76.71	23.27	17.95	12.79	76.27	22.40	14.71	12.15	78.65	31.35
50	50	19.19	13.02	80.47	16.50	17.65	12.62	80.19	15.30	13.86	11.34	81.24	10.82
50	100	14.66	13.02	82.64	17.87	12.90	11.32	77.83	15.69	9.94	10.42	79.03	11.71
100	100	10.18	11.26	81.93	12.26	9.04	10.52	80.97	11.84	5.81	10.24	83.67	7.52

Table 2: Covariate-assisted EB attains the lowest R-MSE for large samples, reaching 73–90% improvement over R-MLE and 3–7× lower MSE than NPMLE in all settings. CAEB (Covariate-assisted EB), SEP (EBMR with a separately exchangeable prior), NPMLE, and EBMF across linear, logistic, and nonlinear generative models. Each cell reports the median R-MSE (lower is better).

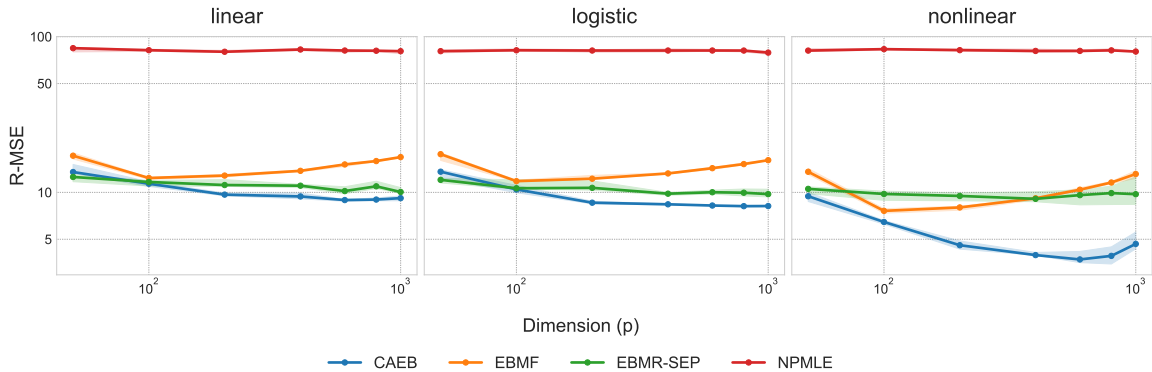


Figure 2: Covariate-assisted EB achieves the lowest risk in large-sample settings. When p is large, all methods achieve constant MSE that reflects the oracle risk as determined by the symmetry group. Covariate-assisted EB achieves the lowest risk compared to other benchmarks.

further shows that with $n = 100$ and p increasing from 100 to 1000, CAEB dominates across all three generative settings.

We also assess the robustness of BEB methods to misspecification of the noise process. Specifically, we rerun the simulations with noise drawn from a t -distribution with degrees of freedom 5 and scale parameter 1 instead of the $N(0, 1)$ distribution. While the absolute MSEs of the methods are slightly higher, the qualitative comparison among the methods is unchanged. See Figure 8 in the Appendix for details.

4.3 Empirical Bayes Spatial Regression

Finally, we evaluate empirical Bayes spatial regression with simulated data. We generate spatial data on an evenly spaced grid $-10 = \omega_1 < \omega_2 < \dots < \omega_n = 10$. The observed variables follow the model

$$x_{\omega_i} = a_{\omega_i}^\top \beta^* + z_{\omega_i}^* + \varepsilon_{\omega_i}, \quad i = 1, \dots, n,$$

with design vectors $a_{\omega_i} = (1, \xi_{\omega_i}) \in \mathbb{R}^p$ where $\xi_{\omega_i} \sim \mathcal{N}(0, I_{p-1})$, and noise $\varepsilon_{\omega_i} \stackrel{iid}{\sim} \mathcal{N}(0, \tau^{-1})$.

We fix $p = 3$ and set $\beta^* = (0.5, -1.2, 0.3)^\top$. The latent field $z^* = (z_{\omega_1}^*, \dots, z_{\omega_n}^*)$ is a stationary Gaussian process with covariance kernel

$$\Sigma_{ij}^* = k_{w, \sigma, \mu}(\omega_i - \omega_j), \quad w = (0.5, 0.3, 0.2), \quad \sigma = (1.0, 0.2, 0.35), \quad \mu = (0, 0.15, -0.25),$$

where the formula for $k_{w, \sigma, \mu}$ is in Eq. 64. Equivalently, it is a stationary kernel with a three-component Gaussian mixture $0.5\mathcal{N}(0, 1^2) + 0.3\mathcal{N}(0.15, 0.2^2) + 0.2\mathcal{N}(-0.25, 0.35^2)$ as the spectral density. We draw a single $z_n^* \sim \mathcal{N}(0, \Sigma^*)$ as the ground truth.

To simulate \mathbf{x}_n , we vary the precision $\tau \in \{0.25, 1, 4\}$ and the sample size n from 100 to 3000. We fit spatial EB regression (§ 3.3) with $K \in \{3, 4, 5\}$, draw posterior samples of β and z_n , and report the posterior mean of z_n and its R-MSE.

As a baseline, we apply the NPMLE to residuals under the true coefficient β^* :

$$r_\omega = x_\omega - a_\omega^\top \beta^*, \quad r_\omega \sim \mathcal{N}(z_\omega^*, \tau_\omega^{-1}),$$

and estimate z_n^* using the normal-means model with a fully exchangeable prior (§ 3.1). The MLE for z_ω in this case is r_ω .

Figure 3 shows the results. EB spatial regression uniformly dominates the regression-adjusted NPMLE, which indicates that stationarity is a more informative symmetry than full exchangeability for this example. At each noise level, the MSE of the EB spatial estimator of z_n^* decreases sharply with the sample size, while the MSE of the regression-adjusted NPMLE remains essentially flat as n increases. The performance of the two methods is comparable only for small samples (e.g., $n = 100$); for larger n , the spatial EB estimator achieves substantially lower error. In Figure 9 of § G, we show that the MSE of the posterior-mean estimator for β also decreases with n under the EB spatial regression model, which suggests that the posterior of β satisfies posterior consistency.

In high-precision regimes, the NPMLE yields little improvement, with its R-MSE hovering around 80. By contrast, the R-MSE of EB spatial regression drops below 20 once $n \geq 2000$, albeit with higher cross-replicate variability than in lower-precision regimes.

5 Real Data Examples

For applications, we consider (i) a semisynthetic study where we add Gaussian noise to a cancer gene–expression matrix with varying noise levels, and (ii) denoising and interpolating NYC air–quality data using EB spatial regression. In the first example, we evaluate our methods using R-MSE of the recovered matrix versus the ground truth. In the second example, we provide the full inference results to reason about the learned prior and posterior.

5.1 Cancer

We apply empirical Bayes matrix recovery methods to a gene–expression dataset under varying levels of noise corruption. The dataset is a 251×226 gene–expression matrix analyzed by [Carvalho et al. \(2008\)](#) and [Knowles and Ghahramani \(2011\)](#), containing

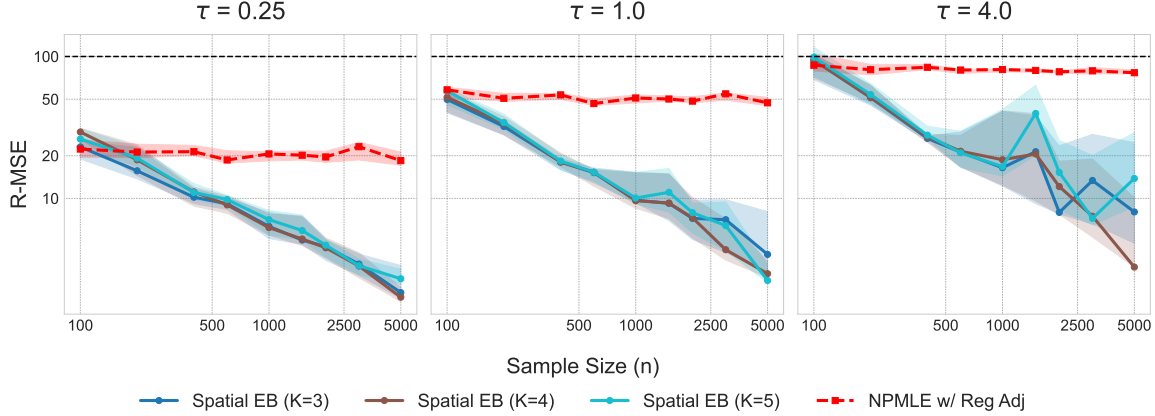


Figure 3: EB spatial regression dominates NPMLE. Relative MSE for recovering the latent series z_n^* across sample size n and noise precision τ . EB spatial regression is fit with $K \in \{3, 4, 5\}$ mixtures and is stable to modest over-specification of K . The NPMLE baseline uses residuals $r_\omega = x_\omega - a_\omega^\top \beta^*$ with $r_\omega \sim \mathcal{N}(z_\omega, \tau_\omega^{-1})$ and a fully exchangeable prior. Points show medians over 10 replicates; bands show the interquartile range (25–75%). EB error decreases with n , whereas NPMLE error remains roughly flat.

measurements of 226 genes across 251 breast–cancer patients. The statistical goal is to recover the latent gene–expression matrix from a noisy observation. It is reasonable to assume *a priori* that genes are exchangeable and patients are exchangeable, so we apply the empirical Bayes matrix recovery method with a separately exchangeable prior to pool information across related gene-specific and patient-specific effects.

In the semisynthetic design, we add independent Gaussian noise with precision $\tau \in \{0.01, 0.03, 0.1, 0.3, 1, 3, 10\}$ to each entry and compare three empirical Bayes procedures: (i) EBMR with a separately exchangeable prior (EBMR–sep), (ii) nonparametric maximum likelihood estimation (NPMLE; [Jiang and Zhang, 2009](#)), and (iii) empirical Bayes matrix factorization (EBMF; [Wang and Stephens, 2021](#)). We measure the performance by the relative mean–squared error (R–MSE) between the recovered and original matrices, averaged over 20 replicates and summarized by the median R–MSE.

For EBMF, we follow [Wang and Stephens \(2021\)](#) by setting $K = 40$. For EBMR–sep, we discretize $[0, 1]$ on a $K = 10$ grid and parameterize g_{sep} as a two–layer ReLU network with 20 hidden units per layer. We train g_{sep} with Adam (learning rate 0.01) on the variational objective in Algorithm 2 over 500 iterations with 50 gradient steps per iteration. The posterior sampling step uses NUTS with 300 warm–up and 300 retained samples (target acceptance probability 0.8). Each EBMR–sep run requires approximately 5 minutes on a GPU; a full noise–level sweep takes two hours on two GPUs.

Figure 4 shows the results. EBMR–sep attains uniformly lower R–MSE than both NPMLE and EBMF, with the performance gap increasing under higher noise. The intuitive reason is that the separately exchangeable prior captures gene-level and patient-level sharing of information in a nonlinear way, whereas the other two methods either ignore the row/column-

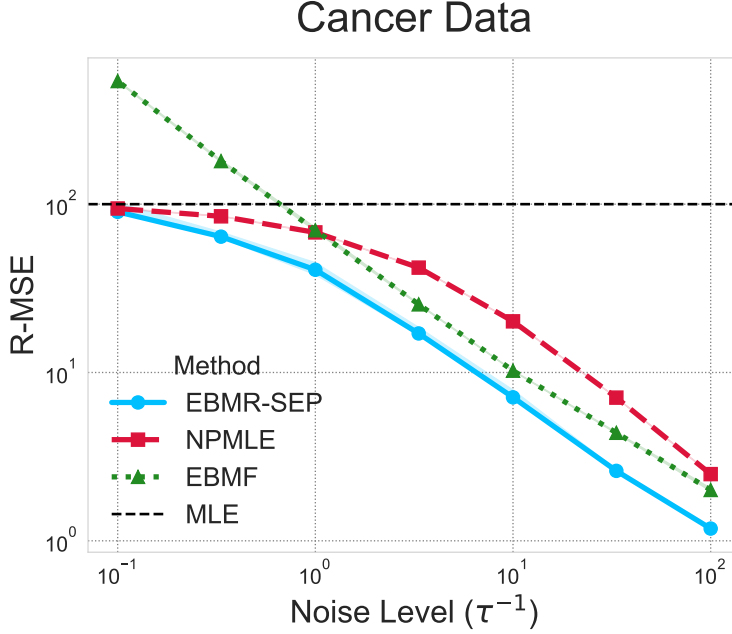


Figure 4: Breast cancer data denoising: EBMR with a separately exchangeable prior achieves the lowest relative MSE across varying noise levels. Scatterplots represent median relative MSE over 10 replicates; bands show the interquartile range (25–75%). There is a “blessing of noise” phenomenon: as the noise level increases, all empirical Bayes methods achieve lower relative MSE.

exchangeable structure (NPMLE) or assume a low-rank structure (EBMF).

5.2 Denoising and Interpolating Air Quality Data in NYC

We apply empirical Bayes spatial regression (SpatialEB) to a dataset on fine particulate matter $\text{PM}_{2.5}$ (in $\mu\text{g}/\text{m}^3$) in New York City. The data comprise hourly readings from 16 monitoring stations obtained from the NYC Department of Health and Mental Hygiene’s Real-Time Air Quality portal.² We focus on four sites—Herald Square, Chinatown, the Lower East Side, and Queens North—using records from January 2019 to May 2025.³ To capture medium-term dynamics, we aggregate to weekly averages $x_{s,t}$ at site s and week t and assign sampling precisions $\tau_{s,t}$ as the inverse within-week variances.

The weekly series contain gaps (outages/maintenance), occasional spikes, and heterogeneous noise. Our goals are to (i) denoise and interpolate the weekly average data for all four sites, (ii) estimate the latent weekly $\text{PM}_{2.5}$ levels with uncertainty quantification, and (iii) characterize the spatio-temporal dependence structure via the fitted spectral density.

We model the data using the spatial regression model

$$x_{s,t} \mid z_{s,t}, \beta \sim \mathcal{N}(z_{s,t} + \beta^\top a_s, \tau_{s,t}^{-1}),$$

where $z_{s,t}$ denotes the latent weekly mean and a_s is a site-specific covariate vector including an intercept and site indicators. The regression component $\beta^\top a_s$ accounts for persistent location effects across monitoring sites. We fit the spatial regression model with $K = 10$ Gaussian-mixture components for the spectral density, then apply the procedure in § E to

²<https://a816-dohbesp.nyc.gov/IndicatorPublic/data-features/realtim-air-quality/>

³We select these four sites because they have the most complete records; for most other sites (including those in Brooklyn, Staten Island, and the Bronx), more than 60% of weekly observations are missing.

obtain posterior means $\hat{z}_{s,t}$, regression coefficients $\hat{\beta}$, 95% credible bands for $\{z_{s,t}\}$, and kriged imputations for missing weeks. We also report site-adjusted means $\hat{m}_{s,t} = \hat{z}_{s,t} + \hat{\beta}^\top a_s$ with credible bands.

When we parameterize the spectral density, $\omega = (\omega_{\text{time}}, \omega_{\text{space}})$ denotes temporal and spatial frequencies. The model learns a spectral density $\psi(\omega)$; by Bochner’s theorem this induces a stationary covariance $k(\Delta)$ in the (t, space) domain. Peaks in $\psi(\omega)$ correspond to dominant temporal cycles and spatial scales of variation in $z_{s,t}$.

We assess the imputation accuracy of EB spatial regression against three Gaussian–process regressors on the same site–week features as our EB model, standardizing inputs and using per–observation noise variances $\alpha_i = \tau_i^{-1}$ from within-week precision. The models differ only by kernel—RBF (squared–exponential, smooth), Matérn ($\nu = 3/2$) (rougher trajectories), and Rational Quadratic (a scale–mixture kernel capturing multi–scale variability)—each with a small white-noise nugget (10^{-3}). Kernel hyperparameters are learned by maximizing the marginal likelihood. On held–out data, we report the MSE of the imputed series against the true weekly averages. Figure 6 shows that EB spatial regression achieves substantially lower MSE than all GP baselines because the fitted spectral density adaptively captures the bimodal spatio–temporal variation. By comparing the four methods, we see that fitting a more flexible prior family that respects the shift invariance yields performance gain in imputation.

Figure 5 shows empirical Bayes posterior means with 95% credible bands. The posterior means shows the shrinkage and pooling effects of EB spatial regression: extreme weekly averages (e.g., mid-2023) are pulled toward the mean. Where observations are dense, the posterior uncertainty around the denoised weekly averages is narrow; where data are missing, it is wider. Within Manhattan (Herald Square, Chinatown, Lower East Side), the model borrows heavily across sites—for example, when Chinatown is entirely missing from mid-2021 to early-2022, the model interpolates from Herald Square and the Lower East Side to produce tight bands; similarly, during mid-2023 to early-2024, the model imputes the Lower East Side using the other two Manhattan sites, which recovers a decreasing, cyclical trend. By contrast, Queens North contributes less to interpolating Manhattan gaps (e.g., mid-2022 to early-2023). The reason for this different shrinking behavior is that the EB model finds two spatio–temporal regimes—one for Manhattan and one for northern Queens; see Figure 10 in § G.4.

6 Discussion

We have presented *Bayesian empirical Bayes*, a general empirical Bayes procedure to obtain accurate simultaneous posterior inference of latent variables when the prior respects a general probabilistic symmetry. Our approach enables the full power of empirical Bayes to be applied to problems with structured data, beyond exchangeable sequences. In this way, it expands the scope of application for EB substantially. Using Bayesian EB, we derived new EB models and inference algorithms for three settings: array data with separate and joint exchangeability, spatial data with shift invariance, and covariate-augmented data.

NYC Weekly Air Quality

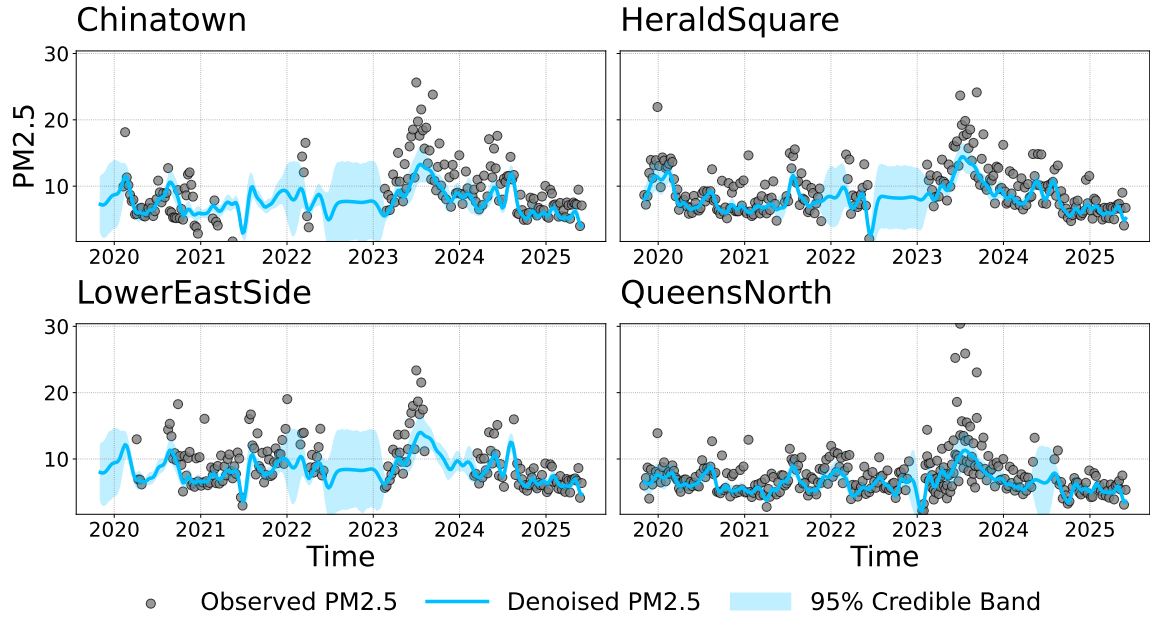


Figure 5: Denoised and interpolated weekly PM_{2.5} in New York City using EB spatial regression. Posterior means with 95% credible bands for three monitoring sites; gray points are observed weekly averages. The model smooths noisy measurements and imputes missing weeks.

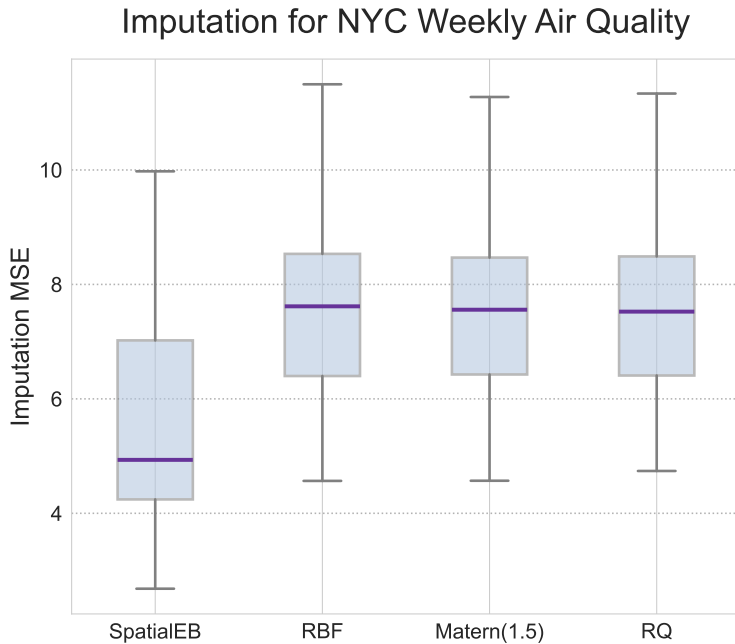


Figure 6: Empirical Bayes spatial regression achieves substantially lower MSE than Gaussian–process baselines. Boxplots show test MSE (median and quantiles) across 50 random masks that hide 20% of observed entries in the NYC air–quality panel. Methods: EB spatial regression with $K = 10$ Gaussian–mixture components for the spectral density, and GPR with RBF, Matérn ($\nu = 3/2$), and Rational–Quadratic kernels.

We demonstrated the competitive performance of Bayesian EB over classical empirical Bayes.

There are several avenues for further research.

First, we have focused here on the derivation and methods behind Bayesian EB. Its theoretical analysis remains an open area. Natural theoretical questions include the identifiability, consistency, and sample complexity of learning the invariant variable g via maximum marginal likelihood and more broadly, estimation under symmetry constraints.

Second, in this paper, we studied symmetry groups based on arrays and spatio-temporal constraints. In many scientific domains, however, the relevant symmetry groups are more complex, such as those arising from physical constraints (e.g., molecular or spacetime symmetries). Another interesting direction is to leverage geometric deep learning (Bronstein et al., 2021) to design new BEB methods tailored to such applications.

Finally, while our initial evidence suggests that Bayesian EB remains competitive under heavy-tailed noise (see Figure 8 in § G.2), it would be valuable to develop sensitivity analysis for these new methods under other types of model misspecification. Sensitivity analysis for empirical Bayes has been studied in Berger and Berliner (1986); Buta and Doss (2011); Doss and Linero (2024).

References

Aldous, D. J. (1981). Representations for partially exchangeable arrays of random variables. *Journal of Multivariate Analysis*, 11.

Aldous, D. J. (2006). Exchangeability and related topics. In *École d'Été de Probabilités de Saint-Flour XIII—1983*, pages 1–198. Springer.

Anderson, M. J. and Robinson, J. (2001). Permutation tests for linear models. *Australian & New Zealand Journal of Statistics*, 43(1):75–88.

Austern, M. and Orbánz, P. (2022). Limit theorems for distributions invariant under groups of transformations. *Annals of Statistics*, 50:1960–1991.

Bachoc, F. (2014). Asymptotic analysis of the role of spatial sampling for covariance parameter estimation of Gaussian processes. *Journal of Multivariate Analysis*, 125.

Banerjee, S., Carlin, B. P., and Gelfand, A. E. (2015). *Hierarchical Modeling and Analysis for Spatial Data*, volume 135 of *Monographs on Statistics and Applied Probability*. CRC Press, Boca Raton, FL, second edition.

Banerjee, S., Gelfand, A. E., Finley, A. O., and Sang, H. (2008). Gaussian predictive process models for large spatial data sets. *Journal of the Royal Statistical Society. Series B: Statistical Methodology*, 70.

Berger, J. and Berliner, L. M. (1986). Robust Bayes and empirical Bayes analysis with ε -contaminated priors. *The Annals of Statistics*, 14.

Berger, J. O., Oliveira, V. D., and Sansó, B. (2001). Objective Bayesian analysis of spatially correlated data. *Journal of the American Statistical Association*, 96.

Bernardo, J.-M. and Smith, A. F. M. (1994). *Bayesian Theory*. Wiley Series in Probability and Mathematical Statistics: Probability and Mathematical Statistics. John Wiley & Sons, Ltd., Chichester.

Bingham, E., Chen, J. P., Jankowiak, M., Obermeyer, F., Pradhan, N., Karaletsos, T., Singh, R., Szerlip, P., Horsfall, P., and Goodman, N. D. (2019). Pyro: Deep universal probabilistic programming. *Journal of Machine Learning Research*, 20.

Blei, D. M., Kucukelbir, A., and McAuliffe, J. D. (2017). Variational inference: A review for statisticians. *Journal of the American Statistical Association*, 112:859–877.

Bochner, S. (2005). *Harmonic Analysis and the Theory of Probability*. Courier Corporation.

Bronstein, M. M., Bruna, J., Cohen, T., and Veličković, P. (2021). Geometric deep learning: Grids, groups, graphs, geodesics, and gauges. *arXiv preprint arXiv:2104.13478*.

Brown, L. and Greenshtein, E. (2009). Nonparametric empirical Bayes and compound decision approaches to estimation of a high-dimensional vector of normal means. *Annals of Statistics*, 37:1685–1704.

Brown, L. D., Mukherjee, G., and Weinstein, A. (2018). Empirical Bayes estimates for a two-way cross-classified model. *Annals of Statistics*, 46.

Buta, E. and Doss, H. (2011). Computational approaches for empirical Bayes methods and bayesian sensitivity analysis. *Annals of Statistics*, 39.

Carbonetto, P. and Stephens, M. (2012). Scalable variational inference for Bayesian variable selection in regression, and its accuracy in genetic association studies. *Bayesian Analysis*, 7:73–108.

Carvalho, C. M., Chang, J., Lucas, J. E., Nevins, J. R., Wang, Q., and West, M. (2008). High-dimensional sparse factor modeling: Applications in gene expression genomics. *Journal of the American Statistical Association*, 103.

Chen, J. (2022). Empirical Bayes when estimation precision predicts parameters. *arXiv preprint arXiv:2212.14444*.

Chen, T., Kornblith, S., Norouzi, M., and Hinton, G. (2020). A simple framework for contrastive learning of visual representations. In *Proceedings of the 37th International Conference on Machine Learning*, pages 1597–1607.

Crane, H. and Towsner, H. (2018). Relatively exchangeable structures. *Journal of Symbolic Logic*, 83.

Deely, J. J. and Lindley, D. V. (1981). Bayes empirical Bayes. *Journal of the American Statistical Association*, 76.

Denault, W. R., Tayeb, K., Carbonetto, P., Willwerscheid, J., and Stephens, M. (2025). Covariate-moderated empirical Bayes matrix factorization. *arXiv preprint arXiv:2505.11639*.

Diaconis, P. (1988). *Group Representations in Probability and Statistics*, volume 11 of *Institute of Mathematical Statistics Lecture Notes—Monograph Series*. Institute of Mathematical Statistics, Hayward, CA.

Doss, H. and Linero, A. (2024). Scalable empirical Bayes inference and bayesian sensitivity analysis. *Statistical Science*, 39.

Eaton, M. L. (1989). *Group Invariance Applications in Statistics*, volume 1 of *Regional Conference Series in Probability and Statistics*. Institute of Mathematical Statistics.

Eden, T. and Yates, F. (1933). On the validity of Fisher's z test when applied to an actual example of non-normal data. *Journal of Agricultural Science*, 23(1):6–17.

Efron, B. (2011). Tweedie's formula and selection bias. *Journal of the American Statistical Association*, 106.

Efron, B. (2012). *Large-scale Inference: Empirical Bayes Methods for Estimation, Testing, and Prediction*, volume 1. Cambridge University Press.

Efron, B. (2014). Two modeling strategies for empirical Bayes estimation. *Statistical Science*, 29.

Efron, B. (2015a). Empirical Bayes deconvolution estimates. *Biometrika*, 103.

Efron, B. (2015b). Frequentist accuracy of Bayesian estimates. *Journal of the Royal Statistical Society Series B: Statistical Methodology*, 77(3):617–646.

Efron, B. (2019). Bayes, oracle Bayes and empirical Bayes. *Statistical Science*, 34:177–201.

Efron, B. (2024). Empirical Bayes: Concepts and methods. In *Handbook of Bayesian, Fiducial, and Frequentist Inference*, pages 8–34. Chapman and Hall/CRC.

Efron, B. and Morris, C. (1971). Limiting the risk of Bayes and empirical Bayes estimators—part i: The Bayes case. *Journal of the American Statistical Association*, 66.

Efron, B. and Morris, C. (1976). Multivariate empirical Bayes and estimation of covariance matrices. *The Annals of Statistics*, 4.

Efron, B., Tibshirani, R., Storey, J. D., and Tusher, V. (2001). Empirical Bayes analysis of a microarray experiment. *Journal of the American Statistical Association*, 96:1151–1160.

Ernst, M. D. (2004). Permutation methods: A basis for exact inference. *Statistical Science*, 19(4):676–685.

Fan, Z., Guan, L., Shen, Y., and Wu, Y. (2023). Gradient flows for empirical bayes in high-dimensional linear models. *arXiv preprint arXiv:2312.12708*.

Finetti, B. D. (1929). Funzione caratteristica di un fenomeno aleatorio. In *Atti del Congresso Internazionale dei Matematici: Bologna del 3 al 10 de settembre di 1928*, pages 179–190.

Fisher, R. A. (1935). *The Design of Experiments*. Oliver and Boyd.

Folland, G. B. (2016). *A Course in Abstract Harmonic Analysis*. CRC press.

Gelman, A., Carlin, J. B., Stern, H. S., and Rubin, D. B. (1995). *Bayesian Data Analysis*. Chapman and Hall/CRC.

Ghosal, S. and van der Vaart, A. (2017). *Fundamentals of Nonparametric Bayesian Inference*, volume 44. Cambridge University Press.

Ghosh, S., Ignatiadis, N., Koehler, F., and Lee, A. (2025). Stein’s unbiased risk estimate and Hyvärinen’s score matching. *arXiv preprint arXiv:2502.20123*.

Giri, N. C. (1996). *Group Invariance in Statistical Inference*. World Scientific.

González, R. E., Muñoz, R. P., and Hernández, C. A. (2018). Galaxy detection and identification using deep learning and data augmentation. *Astronomy and computing*, 25:103–109.

Good, I. (1992). Introduction to Robbins (1955) an empirical Bayes approach to statistics. In *Breakthroughs in Statistics: Foundations and basic theory*, pages 379–387. Springer.

Good, P. I. (2006). *Permutation, Parametric, and Bootstrap Tests of Hypotheses*. Springer Science & Business Media.

Handcock, M. S. and Stein, M. L. (1993). A Bayesian analysis of kriging. *Technometrics*, 35(4):403–410.

Hemerik, J. and Goeman, J. J. (2018). Exact testing with random permutations. *Test*, 27(4):811–825.

Hensman, J., Fusi, N., and Lawrence, N. D. (2013). Gaussian processes for big data. *arXiv preprint arXiv:1309.6835*.

Hoeffding, W. (1952). The large-sample power of tests based on permutations of observations. *The Annals of Mathematical Statistics*, 23(2):169–192.

Hoffman, M. D. and Gelman, A. (2014). The no-U-turn sampler. *Journal of Machine Learning Research*, 15:1593–1623.

Ignatiadis, N. and Huber, W. (2021). Covariate powered cross-weighted multiple testing. *Journal of the Royal Statistical Society. Series B: Statistical Methodology*, 83.

Ignatiadis, N. and Sen, B. (2025a). *Empirical Bayes: From Herbert Robbins to Modern Theory and Applications*. book draft.

Ignatiadis, N. and Sen, B. (2025b). Empirical partially Bayes multiple testing and compound χ^2 decisions. *The Annals of Statistics*, 53(1):1–36.

Ignatiadis, N. and Wager, S. (2019). Covariate-powered empirical Bayes estimation. *Advances in Neural Information Processing Systems*, 32.

Ignatiadis, N. and Wager, S. (2022). Confidence intervals for nonparametric empirical Bayes analysis. *Journal of the American Statistical Association*, 117.

James, W. and Stein, C. (1960). Estimation with quadratic loss. volume 1, page 361. Univ of California Press.

Jiang, W. (2020). On general maximum likelihood empirical Bayes estimation of heteroscedastic iid normal means. *Electronic Journal of Statistics*, 14.

Jiang, W. and Zhang, C.-H. (2009). General maximum likelihood empirical Bayes estimation of normal means. *Annals of Statistics*, 37:1647–1684.

Jiang, W. and Zhang, C.-H. (2010). Empirical Bayes in-season prediction of baseball batting averages. In *Borrowing Strength: Theory Powering Applications–A Festschrift for Lawrence D. Brown*, volume 6, pages 263–274. Institute of Mathematical Statistics.

Kallenberg, O. (1997). *Foundations of Modern Probability*, volume 2. Springer.

Kallenberg, O. (2005). *Probabilistic Symmetries and Invariance Principles*, volume 9. Springer.

Kass, R. E. and Steffey, D. (1989). Approximate Bayesian inference in conditionally independent hierarchical models (parametric empirical Bayes models). *Journal of the American Statistical Association*, 84(407):717–726.

Kennedy, F. E. (1995). Randomization tests in econometrics. *Journal of Business & Economic Statistics*, 13(1):85–94.

Kiefer, J. and Wolfowitz, J. (1956). Consistency of the maximum likelihood estimator in the presence of infinitely many incidental parameters. *The Annals of Mathematical Statistics*, 27:887–906.

Kim, Y., Carbonetto, P., Stephens, M., and Anitescu, M. (2020). A fast algorithm for maximum likelihood estimation of mixture proportions using sequential quadratic programming. *Journal of Computational and Graphical Statistics*, 29.

Kim, Y., Wang, W., Carbonetto, P., and Stephens, M. (2024). A flexible empirical Bayes approach to multiple linear regression, and connections with penalized regression. *Journal of Machine Learning Research*, 25:Paper No. [185], 59.

Kingma, D. P. and Welling, M. (2014). Auto-encoding variational Bayes. In *2nd International Conference on Learning Representations*.

Knowles, D. and Ghahramani, Z. (2011). Nonparametric Bayesian sparse factor models with application to gene expression modeling. *Annals of Applied Statistics*, 5.

Koenker, R. and Mizera, I. (2014). Convex optimization, shape constraints, compound decisions, and empirical Bayes rules. *Journal of the American Statistical Association*, 109:674–685.

LeCun, Y., Bottou, L., Bengio, Y., and Haffner, P. (2002). Gradient-based learning applied to document recognition. *Proceedings of the IEEE*, 86(11):2278–2324.

Lehmann, E. L. (1959). Optimum invariant tests. *The Annals of Mathematical Statistics*, 30.

Lehmann, E. L. and Casella, G. (2006). *Theory of Point Estimation*. Springer Science & Business Media.

Lehmann, E. L. and Stein, C. (1949). On the theory of some non-parametric hypotheses. *The Annals of Mathematical Statistics*, 20(1):28–45.

Li, C., Sun, S., and Zhu, Y. (2024). Fixed-domain posterior contraction rates for spatial Gaussian process model with nugget. *Journal of the American Statistical Association*, 119.

Lindenstrauss, E. (2001). Pointwise theorems for amenable groups. *Inventiones Mathematicae*, 146.

Lindley, D. V. and Smith, A. F. M. (1972). Bayes estimates for the linear model. *Journal of the Royal Statistical Society: Series B (Methodological)*, 34:1–18.

Lloyd, J. R., Orbanz, P., Ghahramani, Z., and Roy, D. M. (2012). Random function priors for exchangeable arrays with applications to graphs and relational data. In *Advances in Neural Information Processing Systems*, volume 2.

Loh, W. L. and Lam, T. K. (2000). Estimating structured correlation matrices in smooth Gaussian random field models. *Annals of Statistics*, 28.

Lubotzky, A. and Segal, D. (2003). *Subgroup growth*, volume 212 of *Progress in Mathematics*. Birkhäuser Verlag, Basel.

Lyle, C., Kwiatkowska, M., and Gal, Y. (2019). An analysis of the effect of invariance on generalization in neural networks. In *ICML Workshop on Understanding and Improving Generalization in Deep Learning*.

Maruyama, G. (1949). The harmonic analysis of stationary stochastic processes. *Memoirs of the Faculty of Science, Kyushu University. Series A, Mathematics*, 4(1):45–106.

Mukherjee, S., Sen, B., and Sen, S. (2023). A mean field approach to empirical Bayes estimation in high-dimensional linear regression. *arXiv preprint arXiv:2309.16843*.

Neal, R. M. (2010). Mcmc using hamiltonian dynamics. *Handbook of Markov Chain Monte Carlo*, 54:113–162.

Oliveira, V. D., Kedem, B., and Short, D. A. (1997). Bayesian prediction of transformed gaussian random fields. *Journal of the American Statistical Association*, 92:1422–1433.

Orbánz, P. and Roy, D. M. (2015). Bayesian models of graphs, arrays and other exchangeable random structures. *IEEE Transactions on Pattern Analysis and Machine Intelligence*, 37.

Pesarin, F. (2001). *Multivariate Permutation Tests: With Applications in Biostatistics*. Wiley.

Pesarin, F. and Salmaso, L. (2010). *Permutation Tests for Complex Data: Theory, Applications and Software*. John Wiley & Sons.

Pesarin, F. and Salmaso, L. (2012). A review and some new results on permutation testing for multivariate problems. *Statistics and Computing*, 22(2):639–646.

Pitman, E. J. G. (1937). Significance tests which may be applied to samples from any populations. *Supplement to the Journal of the Royal Statistical Society*, 4(1):119–130.

Ramdas, A., Barber, R. F., Candès, E. J., and Tibshirani, R. J. (2023). Permutation tests using arbitrary permutation distributions. *Sankhyā A*, 85(2):1156–1177.

Rasmussen, C. E. and Williams, C. K. I. (2006). Gaussian processes for machine learning. *The MIT Press*.

Rizzelli, S., Rousseau, J., and Petrone, S. (2024). Empirical Bayes in Bayesian learning: understanding a common practice. *arXiv preprint arXiv:2402.19036*.

Robbins, H. (1951). Asymptotically subminimax solutions of compound statistical decision problems. In *Proceedings of the Second Berkeley Symposium on Mathematical Statistics and Probability, 1950*, pages 131–148. Univ. California Press, Berkeley-Los Angeles, Calif.

Robbins, H. (1956). An empirical Bayes approach to statistics. In *Proceedings of the Third Berkeley Symposium on Mathematical Statistics and Probability, 1954–1955, vol. I*, pages 157–163. Univ. California Press, Berkeley-Los Angeles, Calif.

Robbins, H. (1980). Estimation and prediction for mixtures of the exponential distribution. *Proceedings of the National Academy of Sciences of the United States of America*, 77.

Robbins, H. and Monro, S. (1951). A stochastic approximation method. *The Annals of Mathematical Statistics*, 22:400–407.

Robert, C. P. (2007). *The Bayesian Choice: from Decision-theoretic Foundations to Computational Implementation*, volume 2. Springer.

Rousseau, J. and Szabo, B. (2017). Asymptotic behaviour of the empirical Bayes posteriors associated to maximum marginal likelihood estimator. *Annals of Statistics*, 45.

Saremi, S. and Hyvärinen, A. (2019). Neural empirical Bayes. *Journal of Machine Learning Research*, 20.

Savage, L. J. (1954). *The Foundations of Statistics*. John Wiley & Sons, Inc., New York; Chapman & Hall, Ltd., London.

Shields, P. C. (1996). *The Ergodic Theory of Discrete Sample Paths*, volume 13. American Mathematical Soc.

Soloff, J. A., Guntuboyina, A., and Sen, B. (2025). Multivariate, heteroscedastic empirical Bayes via nonparametric maximum likelihood. *Journal of the Royal Statistical Society Series B: Statistical Methodology*, 87(1):1–32.

Stein, M. L. (1999). *Interpolation of Spatial Data*. Springer Series in Statistics. Springer-Verlag, New York.

Stephens, M. (2017). False discovery rates: A new deal. *Biostatistics*, 18.

Szabó, B., Vaart, A. V. D., and Zanten, J. V. (2015). Frequentist coverage of adaptive nonparametric Bayesian credible sets. *Annals of Statistics*, 43:1391–1428.

Tan, Z. (2016). Steinized empirical Bayes estimation for heteroscedastic data. *Statistica Sinica*, 26.

Tippe, B., Finucane, H., and Broderick, T. (2021). For high-dimensional hierarchical models, consider exchangeability of effects across covariates instead of across datasets. *Advances in Neural Information Processing Systems*, 34:13471–13484.

Van Handel, R. (2014). Probability in high dimension. *Lecture Notes (Princeton University)*.

Varadarajan, V. S. (1963). Groups of automorphisms of Borel spaces. *Transactions of the American Mathematical Society*, 109.

Wang, G., Sarkar, A., Carbonetto, P., and Stephens, M. (2020). A simple new approach to variable selection in regression, with application to genetic fine mapping. *Journal of the Royal Statistical Society Series B: Statistical Methodology*, 82(5):1273–1300.

Wang, W. and Stephens, M. (2021). Empirical Bayes matrix factorization. *Journal of Machine Learning Research*, 22.

Wijsman, R. A. (1990). *Invariant Measures on Groups and Their Use in Statistics*, volume 14 of *Institute of Mathematical Statistics Lecture Notes—Monograph Series*. Institute of Mathematical Statistics, Hayward, CA.

Wilson, A. G. and Adams, R. P. (2013). Gaussian process kernels for pattern discovery and extrapolation. In *30th International Conference on Machine Learning, ICML 2013*.

Xie, X., Kou, S., and Brown, L. (2012). SURE estimates for a heteroscedastic hierarchical model. *Journal of the American Statistical Association*, 107:1465–1479.

Xu, W. and Stein, M. L. (2017). Maximum likelihood estimation for a smooth Gaussian random field model. *SIAM/ASA Journal on Uncertainty Quantification*, 5.

Yang, C. H., Doss, H., and Vemuri, B. C. (2024). An empirical Bayes approach to shrinkage estimation on the manifold of symmetric positive-definite matrices. *Journal of the American Statistical Association*, 119.

Zhong, X., Su, C., and Fan, Z. (2022). Empirical Bayes PCA in high dimensions. *Journal of the Royal Statistical Society. Series B: Statistical Methodology*, 84.

A Conditions on Groups

We provide the regularity conditions on the group of transformations Φ acting on the space \mathcal{Z}^Ω . For $\phi_1, \phi_2 \in \Phi$, we write the composition $\phi_1\phi_2(\cdot) := \phi_1(\phi_2(\cdot))$. If $\phi \in \Phi$ and $A \subseteq \Phi$, we write $\phi A := \{\phi\psi \mid \psi \in A\}$. If $K, A \subseteq \Phi$, we write $KA := \{\phi\psi \mid \phi \in K, \psi \in A\}$.

We equip Φ with the Borel σ -algebra $\mathcal{B}(\Phi)$. For every locally compact, second countable, and Hausdorff (lcscH) group, there exists a σ -finite measure $|\cdot|$ such that

$$|\phi^{-1}A| = |A|, \quad \text{for all } \phi \in \Phi, A \in \mathcal{B}(\Phi),$$

called a *Haar measure* (Folland, 2016). The Haar measure is unique up to a positive scaling factor. If $A \subset \Phi$ is compact, then $|A|$ is finite.

A *Følner sequence* in Φ is a sequence of compact sets $\mathbf{A}_1, \mathbf{A}_2, \dots$ such that, for every compact subset $K \subset \Phi$,

$$\frac{|K\mathbf{A}_n \cap \mathbf{A}_n|}{|\mathbf{A}_n|} \xrightarrow{n \rightarrow \infty} 1.$$

If Φ is discrete, its compact sets are finite, and hence the condition specializes to the familiar finite Følner property. An lcscH group is called *amenable* if it admits a Følner sequence.

A Følner sequence $\{\mathbf{A}_n\}$ is *tempered* if there is some constant $c > 0$ such that, for all $n \in \mathbb{N}$,

$$|\bigcup_{k < n} \mathbf{A}_k^{-1} \mathbf{A}_n| \leq c |\mathbf{A}_n|.$$

Not every Følner sequence is tempered, but every lcscH group that has a Følner sequence also has a tempered one (Lindenstrauss, 2001, Proposition 1.4).

Finally, we give the definition of a "nice" group, which matches the standard definition in the literature of probabilistic symmetry (Austern and Orbanz, 2022).

Definition 2 (Nice group). *We call Φ a nice group if*

- (i) Φ is a locally compact, second countable, Hausdorff (lcscH) topological group, and the group operations are continuous.
- (ii) Φ is amenable, i.e., it admits a Følner sequence $(\mathbf{A}_n)_{n \in \mathbb{N}}$.

B Empirical Bayes Beyond Index Transformations

In § 2, we assumed Φ to be a group of transformations acting on the index space Ω . There are many interesting groups beyond index transformations, for example the rotation group or the Heisenberg group. We can develop Bayesian empirical Bayes methods for these groups under an equivariant assumption on the likelihood.

Let $\mathbf{x} \in \mathcal{X}^\Omega$ be observed variables and $\mathbf{z} \in \mathcal{X}^\Omega$ local latent variables. A general EB setup is as follows:

$$\mathbf{z} \sim p(\mathbf{z}), \quad \mathbf{x} \sim p(\mathbf{x} | \mathbf{z}).$$

The likelihood $p(\mathbf{x} | \cdot)$ is assumed to be Φ -equivariant in the sense of Definition 4. Specifically,

$$p(\mathbf{x} | \phi(\mathbf{z})) = p(\phi^{-1}(\mathbf{x}) | \mathbf{z}), \quad \forall \phi \in \Phi.$$

As a special case, the product likelihood $p(\mathbf{x} | \mathbf{z}) = \prod_{\omega \in \Omega} p(x_\omega | z_\omega)$ is equivariant with respect to any group of index transformations. The Gaussian likelihood is equivariant to rotations.

By Assumption 1 and Assumption 2, there exists a true prior $p^*(\mathbf{z})$ that is Φ -invariant. If Φ is a nice group in the sense of Definition 2, the ergodic representation theorem holds for Φ . Thus, there exists an invariant variable g such that the population distribution is

$$g \sim \mu^*, \quad \mathbf{z} \sim p(\mathbf{z} | g), \quad \mathbf{x} \sim p(\mathbf{x} | \mathbf{z}). \quad (39)$$

The goal is to compute the posterior $p^*(\mathbf{z} | \mathbf{x})$, given by

$$p^*(\mathbf{z} | \mathbf{x}) \propto \int_{\mathcal{G}} p(\mathbf{x} | \mathbf{z}) p(\mathbf{z} | g) d\mu^*(g).$$

The next result shows that both the population posterior $p^*(\mathbf{z} | \mathbf{x})$ and the population empirical Bayes posterior $p(\mathbf{z} | \mathbf{x}, \hat{g})$ satisfy the equivariance property.

Proposition 3. *The population posterior $p^*(\mathbf{z} | \mathbf{x})$ is a Φ -equivariant conditional distribution, in the sense that for any $\phi \in \Phi$,*

$$p^*(\phi^{-1}(\mathbf{z}) | \mathbf{x}) = p^*(\mathbf{z} | \phi(\mathbf{x})).$$

For any $g \in \mathcal{G}$, the conditional posterior $p(\mathbf{z} | \mathbf{x}, g)$ is also Φ -equivariant, including the population EB posterior $p(\mathbf{z} | \mathbf{x}, \hat{g})$.

This result shows that transforming the structured variable \mathbf{z} by ϕ under the posterior is equivalent to computing the posterior of \mathbf{z} after applying the transformation ϕ to the observed variables \mathbf{x} .

Proof. We first consider the population posterior $p^*(\mathbf{z} | \mathbf{x})$. For any $\phi \in \Phi$,

$$\begin{aligned} p^*(\phi(\mathbf{z}) | \mathbf{x}) &= \int_{\mathcal{G}} p(\mathbf{x} | \phi(\mathbf{z})) p(\phi(\mathbf{z}) | g) d\mu^*(g) \\ &= \int_{\mathcal{G}} p(\mathbf{x} | \phi(\mathbf{z})) p(\mathbf{z} | g) d\mu^*(g) \\ &= \int_{\mathcal{G}} p(\phi^{-1}(\mathbf{x}) | \mathbf{z}) p(\mathbf{z} | g) d\mu^*(g) = p^*(\mathbf{z} | \phi^{-1}(\mathbf{x})). \end{aligned}$$

The second equality follows from the Φ -invariance of $p(\mathbf{z} | g)$, and the third from the Φ -equivariance of the likelihood $p(\mathbf{x} | \mathbf{z})$. An identical argument applies to $p(\mathbf{z} | \mathbf{x}, g)$ for any fixed $g \in \mathcal{G}$, and therefore also to the EB posterior $p(\mathbf{z} | \mathbf{x}, \hat{g})$, where \hat{g} denotes the maximum marginal likelihood estimator. \square

The result suggests that “transform then condition” and “condition then transform” commute for the posterior. The population posterior mean $\mathbb{E}[\mathbf{z} | \mathbf{x}] := \int_{\mathcal{X}^\Omega} \mathbf{z} p^*(\mathbf{z} | \mathbf{x}) d\mathbf{z}$ therefore satisfies $\mathbb{E}[\phi(\mathbf{z}) | \mathbf{x}] = \mathbb{E}[\mathbf{z} | \phi(\mathbf{x})]$ for any $\phi \in \Phi$ when Φ is a group of isometries. This suggests that, to learn the population Bayes estimator of transformed latent variables, it suffices to compute the posterior on transformed datasets. This observation connects empirical Bayes point estimation (Jiang and Zhang, 2009) to the common machine learning practice of enforcing symmetry via data augmentation (González et al., 2018; Lyle et al., 2019; Chen et al., 2020).

C Support Results

Definition 3. A space Ω is *exhaustible by compact sets* if, for every open set $U \subseteq \Omega$, there exists an increasing sequence of compact subsets $S_1 \subseteq S_2 \subseteq \dots$ such that

$$U = \bigcup_{n=1}^{\infty} S_n,$$

and, for every n , S_n is contained in the interior of S_{n+1} .

Definition 4 (Φ -equivariance). A function $t : \mathcal{X}^\Omega \rightarrow \mathcal{X}^\Omega$ is Φ -equivariant if

$$\phi(t(\mathbf{x})) = t(\phi(\mathbf{x})), \quad \text{for all } \phi \in \Phi. \tag{40}$$

Intuitively, a function t is Φ -equivariant if every action of Φ “commutes” with t . An equivariant function t preserves Φ -invariance, as $\phi(\mathbf{x}) \stackrel{d}{=} \mathbf{x}$ implies

$$\phi(t(\mathbf{x})) = t(\phi(\mathbf{x})) \stackrel{d}{=} t(\mathbf{x}).$$

D Algorithms for Empirical Bayes Matrix Recovery

This appendix details the inference algorithms for the empirical Bayes matrix-recovery methods introduced in § 3. § D.1 presents a *variational* procedure for matrix recovery under

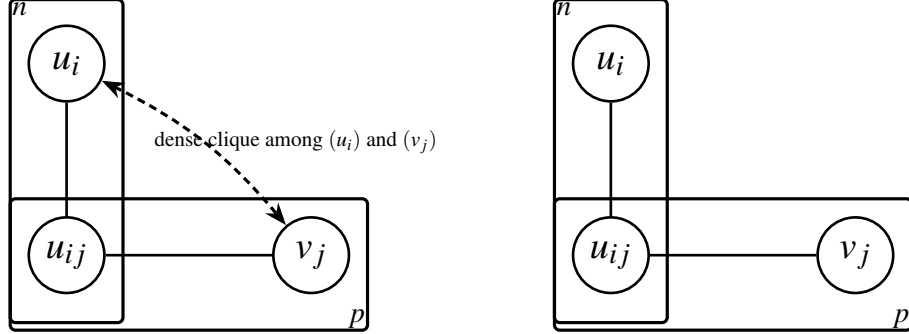


Figure 7: Variational approximation. *Left:* exact posterior with a dense clique among (u_i) and (v_j) and local connections to u_{ij} . *Right:* variational family $q \in \mathcal{Q}_{\text{sep}}$ factorizes across (u_i) and (v_j) while preserving the local chain $u_i—u_{ij}—v_j$.

a separately exchangeable prior (EBMR–sep; Algorithm 2). § D.2 develops the inference algorithm for EBMR with a jointly exchangeable prior (EBMR–joint; Algorithm 3), and § D.3.1 provides the algorithm for covariate-assisted EB (CAEB) which is analogous to the separately exchangeable case.

For all three algorithms, we use variational inference (Blei et al., 2017) to approximate the nonparametric maximum marginal likelihood.

Variational MMLE. Let $\mathcal{Q} \subseteq \mathcal{P}(\mathcal{X}^{S_n})$ be a family of distributions. By the Gibbs variational principle (Van Handel, 2014, Lemma 4.10), one can lower bound the marginal likelihood by

$$\log p(\mathbf{x}_n | g) \geq -\ell(\mathbf{x}_n; g) := \sup_{q \in \mathcal{Q}} \mathbb{E}_{q(\mathbf{z}_n)} [\log p(\mathbf{x}_n | \mathbf{z}_n) + \log p(\mathbf{z}_n | g) - \log q(\mathbf{z}_n)], \quad (41)$$

where $-\ell(\mathbf{x}_n; g)$ is the maximum evidence lower bound (ELBO) over the family \mathcal{Q} .

D.1 EBMR with a Separately Exchangeable Prior

To approximate the intractable marginal likelihood in Eq. 30, we posit the following structured variational family

$$\mathcal{Q}_{\text{sep}} = \left\{ q \in \mathcal{P}([0, 1]^{n+p+np}) : q(\mathbf{u}_{n,p}) = \prod_{i=1}^n q_{\mathbf{u},i}(u_i) \prod_{j=1}^p q_{\mathbf{v},j}(v_j) \prod_{i,j} q_{i,j}(u_{ij} | u_i, v_j) \right\}. \quad (42)$$

Figure 7 motivates \mathcal{Q}_{sep} . In the exact posterior $p(\mathbf{u}_{n,p} | \hat{g}_{\text{sep}}, \mathbf{x}_{n,p})$, the variables $(u_i)_{i \in [n]}$ and $(v_j)_{j \in [p]}$ form a dense clique, while each u_{ij} connects only to (u_i, v_j) . Our variational family replaces the dense clique with a product measure over (u_i) and (v_j) while preserving the local $u_i—u_{ij}—v_j$ chains.

Maximizing the ELBO over \mathcal{Q}_{sep} yields a lower bound of the marginal likelihood,

$$\log p(\mathbf{x}_{n,p} | g_{\text{sep}}) \geq \sup_{q \in \mathcal{Q}_{\text{sep}}} \text{ELBO}(q, g_{\text{sep}}) := \sup_{q \in \mathcal{Q}_{\text{sep}}} \mathbb{E}_{q(\mathbf{u}_{n,p})} [\log p(\mathbf{x}_{n,p} | g_{\text{sep}}, \mathbf{u}_{n,p}) - \log q(\mathbf{u}_{n,p})].$$

Let $q_{\mathbf{u}} = \bigotimes_{i=1}^n q_{\mathbf{u},i}$ and $q_{\mathbf{v}} = \bigotimes_{j=1}^p q_{\mathbf{v},j}$. We estimate g_{sep} by minimizing the variational loss

$$\hat{g}_{\text{sep}} \in \arg \min_{g_{\text{sep}} \in \mathcal{G}} \ell(\mathbf{x}_{n,p}; g_{\text{sep}}) := - \sup_{q \in \mathcal{Q}_{\text{sep}}} \text{ELBO}(q, g_{\text{sep}}). \quad (43)$$

A direct calculation (see § F.2) shows that

$$\begin{aligned} \ell(\mathbf{x}_{n,p}; g_{\text{sep}}) = \inf_{q_{\mathbf{u}} \in \mathcal{P}([0,1])^{\otimes n}, q_{\mathbf{v}} \in \mathcal{P}([0,1])^{\otimes p}} & \left\{ - \sum_{i=1}^n \sum_{j=1}^p \mathbb{E}_{q_{\mathbf{u},i}(u_i) q_{\mathbf{v},j}(v_j)} \left[\text{LSE}(x_{ij}, \tau_{ij}, u_i, v_j, g_{\text{sep}}) \right] \right. \\ & \left. + \sum_{i=1}^n \mathbb{E}_{q_{\mathbf{u},i}(u_i)} [\log q_{\mathbf{u},i}(u_i)] + \sum_{j=1}^p \mathbb{E}_{q_{\mathbf{v},j}(v_j)} [\log q_{\mathbf{v},j}(v_j)] \right\}, \end{aligned} \quad (44)$$

where $\text{LSE}(X, \tau, U, V, g_{\text{sep}}) := \log \int_0^1 \exp \left(-\frac{\tau}{2} (X - g_{\text{sep}}(U, V, u))^2 \right) du$.

Alternating optimization. To fit the variational distributions, we discretize $q_{\mathbf{u},i}$ and $q_{\mathbf{v},j}$ on the $(K+1)$ -point grid $u_k := k/K$ for $k = 0, \dots, K$ over $[0, 1]$:

$$q_{\mathbf{u},i} = \sum_{k=0}^K w_{\mathbf{u},ik} \delta_{u_k}, \quad q_{\mathbf{v},j} = \sum_{k=0}^K w_{\mathbf{v},jk} \delta_{u_k}, \quad \text{where } u_k = k/K, \quad \sum_{k=0}^K w_{\bullet,k} = 1. \quad (45)$$

Following Eq. 44, the empirical Bayes estimate minimizes the negative ELBO over the network and grid weights:

$$\begin{aligned} (\hat{g}_{\text{sep}}, \hat{\mathbf{w}}_{\mathbf{u}}, \hat{\mathbf{w}}_{\mathbf{v}}) \in \arg \min_{g_{\text{sep}} \in \mathcal{G}_{\text{NN}}, \mathbf{w}_{\mathbf{u}}, \mathbf{w}_{\mathbf{v}} \in \Delta_{K+1}} & \left\{ - \sum_{i=1}^n \sum_{j=1}^p \sum_{k=0}^K \sum_{k'=0}^K w_{\mathbf{u},ik} w_{\mathbf{v},jk'} \widehat{\text{LSE}}(x_{ij}, \tau_{ij}, u_k, u_{k'}, g_{\text{sep}}) \right. \\ & \left. + \sum_{i=1}^n \sum_{k=0}^K w_{\mathbf{u},ik} \log w_{\mathbf{u},ik} + \sum_{j=1}^p \sum_{k=0}^K w_{\mathbf{v},jk} \log w_{\mathbf{v},jk} \right\}, \end{aligned} \quad (46)$$

where $\widehat{\text{LSE}}(x, \tau, u, v, g_{\text{sep}}) := \log \sum_{k=0}^K \exp \left\{ -\frac{\tau}{2} (x - g_{\text{sep}}(u, v, k/K))^2 \right\} - \log(K+1)$.

We minimize (46) by applying a block-coordinate descent algorithm: (i) update the row weights $\{\mathbf{w}_{\mathbf{u},i}\}$, (ii) update the column weights $\{\mathbf{w}_{\mathbf{v},j}\}$, (iii) update the network parameters of g_{sep} by stochastic gradient descent (Adam; [Kingma and Welling, 2014](#)). Algorithm 2 provides the explicit updates. The weight updates can be parallelized over i and j . Each iteration costs $O(npK^2)$ time and $O((n+p)K)$ memory.

Algorithm 2: EBMR with a Separately Exchangeable Prior (EBMR-sep)

Input: Data matrix $\mathbf{x}_{n,p}$, precision matrix $\boldsymbol{\tau}_{n,p}$, neural network class \mathcal{G}_{NN} , grid size K , tuning parameters (epochs, learning rate)

Initialize: neural network parameters; probability weights

$$\mathbf{w}_{\mathbf{u},1}, \dots, \mathbf{w}_{\mathbf{u},n}, \mathbf{w}_{\mathbf{v},1}, \dots, \mathbf{w}_{\mathbf{v},p} \in \Delta_{K+1}.$$

repeat

for $i = 1$ **to** n (parallelizable) **do**

$$\rho_{\mathbf{u},ik} \leftarrow \sum_{j=1}^p \sum_{k_2=0}^K w_{\mathbf{v},jk_2} \widehat{\text{LSE}}(x_{ij}, \tau_{ij}, u_k, u_{k_2}, \mathbf{g}_{\text{sep}}), \quad k = 0, \dots, K,$$

$$\mathbf{w}_{\mathbf{u},i} \leftarrow \text{SOFTMAX}(\rho_{\mathbf{u},i0}, \dots, \rho_{\mathbf{u},iK}).$$

end

for $j = 1$ **to** p (parallelizable) **do**

$$\rho_{\mathbf{v},jk} \leftarrow \sum_{i=1}^n \sum_{k_1=0}^K w_{\mathbf{u},ik_1} \widehat{\text{LSE}}(x_{ij}, \tau_{ij}, u_{k_1}, u_k, \mathbf{g}_{\text{sep}}), \quad k = 0, \dots, K,$$

$$\mathbf{w}_{\mathbf{v},j} \leftarrow \text{SOFTMAX}(\rho_{\mathbf{v},j0}, \dots, \rho_{\mathbf{v},jK}).$$

end

Update the neural network parameters by stochastic gradient descent:

$$\mathbf{g}_{\text{sep}} \leftarrow \arg \max_{\mathbf{g}_{\text{sep}} \in \mathcal{G}_{\text{NN}}} \sum_{i=1}^n \sum_{j=1}^p \sum_{k_1=0}^K \sum_{k_2=0}^K w_{\mathbf{u},ik_1} w_{\mathbf{v},jk_2} \widehat{\text{LSE}}(x_{ij}, \tau_{ij}, u_{k_1}, u_{k_2}, \mathbf{g}_{\text{sep}}).$$

until convergence;

Output: Fitted weights $\mathbf{w}_{\mathbf{u},1}, \dots, \mathbf{w}_{\mathbf{u},n}, \mathbf{w}_{\mathbf{v},1}, \dots, \mathbf{w}_{\mathbf{v},p}$ and network \mathbf{g}_{sep} .

Proposition 4. *Algorithm 2 performs block-coordinate ascent on the variational inference problem (46).*

Approximate posterior computation. The last step of Algorithm 1 is to sample from the empirical Bayes posterior

$$\hat{p}(\mathbf{z}_n \mid \mathbf{x}_n) \propto p(\mathbf{x}_n \mid \mathbf{z}_n) p(\mathbf{z}_n \mid \hat{\mathbf{g}}). \quad (47)$$

We take the default sampler to be the No-U-Turn Sampler (NUTS) (Hoffman and Gelman, 2014), an adaptive variant of Hamiltonian Monte Carlo (Neal, 2010) implemented in the Pyro probabilistic programming package (Bingham et al., 2019). NUTS automatically tunes the step size and trajectory length parameters. We run NUTS for a fixed number of iterations that includes an initial warmup phase and thinning. When the full MCMC fails to converge, an alternative is to draw surrogate samples from variational approximation $\hat{q}(\mathbf{z}_n)$ obtained in Algorithm 2. This requires using the fitted variational distributions from Algorithm 2 to approximately sample from the posterior $p(\mathbf{z}_{n,p} \mid \hat{\mathbf{g}}_{\text{sep}}, \mathbf{x}_{n,p})$. Suppose that Algorithm 2 returns $\hat{q}_{\mathbf{u},i} = \sum_{k=0}^K \hat{w}_{\mathbf{u},ik} \delta_{u_k}$ and $\hat{q}_{\mathbf{v},j} = \sum_{k=0}^K \hat{w}_{\mathbf{v},jk} \delta_{u_k}$. To sample z_{ij} , we first draw $u_i \sim \hat{q}_{\mathbf{u},i}$

and $v_j \sim \hat{q}_{v,j}$. Conditional on (u_i, v_j) , we draw $u_{ij} \in \{0, 1/K, \dots, 1\}$ with probability

$$\hat{q}_{ij}(u_{ij} = k/K \mid u_i, v_j, \mathbf{x}_{n,p}) = \frac{\exp\left\{-\frac{\tau_{ij}}{2}(x_{ij} - \hat{g}_{\text{sep}}(u_i, v_j, k/K))^2\right\}}{\sum_{\ell=0}^K \exp\left\{-\frac{\tau_{ij}}{2}(x_{ij} - \hat{g}_{\text{sep}}(u_i, v_j, \ell/K))^2\right\}}, \quad k = 0, \dots, K.$$

This yields a sample $z_{ij} = \hat{g}_{\text{sep}}(u_i, v_j, u_{ij})$ from the variational posterior.

D.2 EBMR with a Jointly Exchangeable Prior

We now develop empirical Bayes matrix recovery under a jointly exchangeable prior. Assume that Assumption 1 and Assumption 2 hold with the true prior being jointly exchangeable. By the Aldous–Hoover theorem, the population distribution for \mathbf{x} has the form

$$g_{\text{joint}} \sim \mu^*, \quad (48)$$

$$u_i, u_{ij} \stackrel{iid}{\sim} \text{unif}[0, 1], \quad (49)$$

$$z_{ij} = g_{\text{joint}}(u_i, u_j, u_{ij}), \quad (50)$$

$$x_{ij} \sim \mathcal{N}\left(z_{ij}, \tau_{ij}^{-1}\right), \quad (i, j) \in \mathbb{N}^2. \quad (51)$$

For finite population, we require the observed matrix to have the same number of rows and columns to apply joint exchangeability. For $n \geq 1$, let $\mathbf{x}_n = (x_{\omega})_{\omega \in [n]^2}$ denote an observed $n \times n$ matrix. By Proposition 1, \mathbf{x}_n follows the marginal distribution of (49)–(51) on the index set $S_n = [n]^2$.

Let $\mathbf{z}_n = (z_{\omega})_{\omega \in S_n}$ denote the corresponding local latent variables. For the invariant variable g_{joint} , the conditional distribution $p(\mathbf{z}_n \mid g_{\text{joint}})$ is given by (49)–(50). By Proposition 1, the finite-sample generative process is described by the same equations (48)–(51) with $(i, j) \in [n]^2$.

D.2.1 Fitting procedure

Let $\mathbf{u}_n = (u_i, u_{ij})_{(i,j) \in [n]^2}$ denote the set of row-specific and entry-specific latent variables. Algorithm 1 estimates \hat{g}_{joint} by maximizing the marginal likelihood

$$\log p(\mathbf{x}_n \mid g_{\text{joint}}) := \log \int_{[0,1]^{n+n^2}} \prod_{i=1}^n \prod_{j=1}^n p(x_{ij} \mid g_{\text{joint}}(u_i, u_j, u_{ij})) \, d\mathbf{u}_n. \quad (52)$$

Directly maximizing the marginal likelihood over all functions $g_{\text{joint}} : [0, 1]^3 \mapsto \mathbb{R}$ is intractable, due to the $(n + n^2)$ -dimensional integral. So we approximate the integral using variational inference.

D.2.2 Variational approximation

Consider the posterior $p(\mathbf{u}_n \mid \mathbf{x}_n, g_{\text{joint}})$ under model (49)–(51).

In the exact posterior $p(\mathbf{u}_n \mid \mathbf{x}_n, \mathbf{g}_{\text{joint}})$, the variables $(u_{ij})_{i,j \in [n]}$ are conditionally independent given $(u_i)_{i \in [n]}$. To capture the graphical structure locally, we posit the variational family

$$\mathcal{Q}_{\text{joint}} = \left\{ \mathbf{q} : \mathbf{q}(\mathbf{u}_n) = \prod_{i=1}^n \mathbf{q}_{\mathbf{u},i}(u_i) \prod_{i,j} \mathbf{q}_{i,j}(u_{ij} \mid u_i, u_j) \right\}. \quad (53)$$

Let $\mathbf{q}_{\mathbf{u}} = \bigotimes_{i=1}^n \mathbf{q}_{\mathbf{u},i}$. The variational method maximizes the evidence lower bound (ELBO) subject to $\mathbf{q} \in \mathcal{Q}_{\text{joint}}$.

Proposition 5. *Let \mathcal{Q} be the variational family in (53). The variational loss for $\mathbf{g}_{\text{joint}}$ is*

$$\begin{aligned} \ell(\mathbf{x}_n; \mathbf{g}_{\text{joint}}) := \inf_{\mathbf{q}_{\mathbf{u}} \in \mathcal{P}([0,1])^{\otimes n}} & \left\{ - \sum_{i=1}^n \sum_{j=1}^n \mathbb{E}_{\mathbf{q}_{\mathbf{u},i}(u_i) \mathbf{q}_{\mathbf{u},j}(u_j)} [\text{LSE}(x_{ij}, \tau_{ij}, u_i, u_j, \mathbf{g}_{\text{joint}})] \right. \\ & \left. + \sum_{i=1}^n \mathbb{E}_{\mathbf{q}_{\mathbf{u},i}(u_i)} [\log \mathbf{q}_{\mathbf{u},i}(u_i)] \right\}, \end{aligned} \quad (54)$$

where

$$\text{LSE}(x_{ij}, \tau_{ij}, u_i, u_j, \mathbf{g}_{\text{joint}}) := \log \int_0^1 \exp\left(-\frac{\tau_{ij}}{2} [x_{ij} - \mathbf{g}_{\text{joint}}(u_i, u_j, u)]^2\right) du.$$

We parametrize $\mathbf{g}_{\text{joint}}$ with a neural network class \mathcal{G}_{NN} and fit it by minimizing the variational loss:

$$\hat{\mathbf{g}}_{\text{joint}} \in \arg \min_{\mathbf{g}_{\text{joint}} \in \mathcal{G}_{\text{NN}}} \ell(\mathbf{x}_n; \mathbf{g}_{\text{joint}}). \quad (55)$$

Since $\mathbf{q}_{\mathbf{u},i} \in \mathcal{P}([0,1])$, we discretize it as

$$\mathbf{q}_{\mathbf{u},i} = \sum_{k=0}^K w_{ik} \delta_{u_k}, \quad u_k = \frac{k}{K}, \quad \sum_{k=0}^K w_{ik} = 1.$$

Algorithm 3 implements EBMR with a jointly exchangeable prior.

With the estimated function $\hat{\mathbf{g}}_{\text{joint}}$ from Algorithm 3, we use the No-U-Turn sampler (NUTS) to sample from the posterior $p(z_{ij} \mid \hat{\mathbf{g}}_{\text{joint}}, \mathbf{x}_n)$ of the EBMR model, given by

$$(u_i, u_j, u_{ij}) \sim p(u_i, u_j, u_{ij} \mid \mathbf{x}_n, \hat{\mathbf{g}}_{\text{joint}}), \quad z_{ij} = \hat{\mathbf{g}}_{\text{joint}}(u_i, u_j, u_{ij}). \quad (56)$$

Algorithm 3: EBMR with a Jointly Exchangeable Prior (EBMR–Joint)

Input: Data matrix \mathbf{x}_n , precision matrix $\tau_n = (\tau_{ij})_{i,j \in [n]}$, network class \mathcal{G}_{NN} , grid size K , optimization hyperparameters (epochs, learning rate)

Initialize: network $\mathbf{g}_{\text{joint}} \in \mathcal{G}_{\text{NN}}$; weights $\mathbf{w}_1, \dots, \mathbf{w}_n \in \Delta_{K+1}$.

repeat

for $i = 1$ **to** n (parallelizable) **do**

$$\rho_{ik} \leftarrow \widehat{\text{LSE}}\left(x_{ii}, \tau_{ii}, u_k, u_k, \mathbf{g}_{\text{joint}}\right) + \sum_{j \neq i} \sum_{k_2=0}^K w_{jk_2} \widehat{\text{LSE}}\left(x_{ij}, \tau_{ij}, u_k, u_{k_2}, \mathbf{g}_{\text{joint}}\right), \quad k = 0, \dots, K,$$

$$\mathbf{w}_i \leftarrow \text{SOFTMAX}(\rho_{i0}, \dots, \rho_{iK}).$$

end

Update the neural network parameters with stochastic gradient ascent:

$$\mathbf{g}_{\text{joint}} \leftarrow \arg \max_{\mathbf{g} \in \mathcal{G}_{\text{NN}}} \sum_{i=1}^n \sum_{k=0}^K w_{ik} \left[\widehat{\text{LSE}}(x_{ii}, \tau_{ii}, u_k, u_k, \mathbf{g}) + \sum_{j \neq i} \sum_{k_2=0}^K w_{jk_2} \widehat{\text{LSE}}(x_{ij}, \tau_{ij}, u_k, u_{k_2}, \mathbf{g}) \right].$$

until convergence;

Output: Fitted weights $\mathbf{w}_1, \dots, \mathbf{w}_n$ and network $\mathbf{g}_{\text{joint}}$.

Corollary 1. *Algorithm 2 performs block–coordinate ascent on the variational inference problem (46).*

D.3 Covariate-Assisted Empirical Bayes

We extend empirical Bayes matrix recovery with a separately exchangeable prior to incorporate covariates on rows and columns. Let $\Omega = \mathbb{N}^2$ and $\mathcal{X} = \mathbb{R}$. We observe a matrix $\mathbf{x}_{n,p} = (x_{ij})_{(i,j) \in [n] \times [p]}$ with row covariates $\mathbf{y}_n = (y_i)_{i=1}^n$ with $y_i \in \mathcal{Y}$ and column covariates $\mathbf{a}_p = (a_j)_{j=1}^p$ with $a_j \in \mathcal{A}$, generated via

$$x_{ij} \sim \mathcal{N}(z_{ij}, \tau_{ij}^{-1}), \quad \tau_{ij} > 0.$$

The statistical goal is to recover the latent array $\mathbf{z}_{n,p}$. On the population level, we impose *relative exchangeability* with respect to the observed covariates: the infinite array \mathbf{z} is said to be \mathbf{y} – \mathbf{a} exchangeable if its law is invariant under relabelings that preserve covariate values,

$$\Phi_{\mathbf{y}, \mathbf{a}} := \{\sigma \in \mathbb{S} : y_{\sigma(i)} = y_i \forall i\} \times \{\pi \in \mathbb{S} : a_{\pi(j)} = a_j \forall j\}.$$

Under \mathbf{y} – \mathbf{a} exchangeability, an extension of Aldous–Hoover theorem yields a measurable representation (Crane and Towsner, 2018): there exists a random function $\mathbf{g}_{\text{rel}} : \mathcal{Y} \times \mathcal{A} \times [0, 1]^3 \rightarrow \mathbb{R}$ such that, for iid $u_i, v_j, u_{ij} \sim \text{unif}[0, 1]$,

$$u_i, v_j, u_{ij} \stackrel{iid}{\sim} \text{unif}[0, 1], \quad z_{ij} = \mathbf{g}_{\text{rel}}(y_i, a_j, u_i, v_j, u_{ij}).$$

The covariate-assisted array model is

$$u_i, v_j, u_{ij} \stackrel{iid}{\sim} \text{unif}[0, 1], \quad z_{ij} = g_{\text{rel}}(y_i, a_j, u_i, v_j, u_{ij}), \quad x_{ij} \sim \mathcal{N}\left(z_{ij}, \tau_{ij}^{-1}\right). \quad (57)$$

We call the Bayesian empirical Bayes method for this model *covariate-assisted empirical Bayes* (CAEB). The estimation procedure mirrors EBMR with a separately exchangeable prior: we maximize a variational lower bound to the marginal likelihood over a structured family for (u_i, v_j, u_{ij}) . We parameterize the invariant variable g_{rel} as a neural network that takes $(y_i, a_j, u_i, v_j, u_{ij})$ as inputs. With \hat{g}_{rel} in hand, we draw from the plug-in posterior $p(\mathbf{z}_{n,p} | \hat{g}_{\text{rel}}, \mathbf{x}_{n,p})$. In the next section, we derive the variational lower bound to learn the invariant variable g_{rel} .

Related approaches include the covariate-assisted EB method of [Ignatiadis and Wager \(2019\)](#), which fits a normal-means sequence model with the prior's mean and variance modeled as functions of covariates, and [Denault et al. \(2025\)](#), which develops covariate-assisted empirical Bayes matrix factorization. In the latter model, the loading and factor components each follow i.i.d. priors parameterized by row/column covariates.

D.3.1 Fitting procedure

Let $\mathbf{u}_{n,p} := (u_i, v_j, u_{ij})_{(i,j) \in [n] \times [p]}$. To follow Algorithm 1, the inference steps of covariate-assisted EB involve

1. Compute \hat{g}_{rel} by maximizing the marginal likelihood

$$\log p(\mathbf{x}_{n,p} | g_{\text{rel}}) := \log \int_{[0,1]^{n+p+np}} \exp \left\{ - \sum_{i=1}^n \sum_{j=1}^p \frac{\tau_{ij}}{2} [x_{ij} - g_{\text{rel}}(y_i, a_j, u_i, v_j, u_{ij})]^2 \right\} d\mathbf{u}_{n,p}. \quad (58)$$

2. Sample z_{ij} from the posterior $p(z_{ij} | \hat{g}_{\text{rel}}, \mathbf{x}_{n,p})$ for $i \in [n]$ and $j \in [p]$.

As in EBMR–sep, the MMLE in (58) is intractable for large n, p . We therefore adopt the same structured variational family \mathcal{Q}_{sep} from (42) for the latent variables $\mathbf{u}_{n,p}$ and discretize each variational marginal on a K -point grid over $[0, 1]$. We parameterize g_{rel} with a neural network class \mathcal{G}_{NN} and minimize the variational loss

$$\hat{g}_{\text{rel}} \in \arg \min_{g_{\text{rel}} \in \mathcal{G}_{\text{NN}}} \ell(\mathbf{x}_{n,p}; g_{\text{rel}}),$$

where, with discretized weights,

$$\begin{aligned} \ell(\mathbf{x}_{n,p}; g_{\text{rel}}) = & \inf_{\mathbf{w}_{\mathbf{u}}, \mathbf{w}_{\mathbf{v}} \in \Delta_{K+1}} \left\{ - \sum_{i=1}^n \sum_{j=1}^p \sum_{k=0}^K \sum_{k'=0}^K \mathbf{w}_{\mathbf{u},ik} \mathbf{w}_{\mathbf{v},jk'} \text{LSE} \left(x_{ij}, \tau_{ij}, y_i, a_j, \frac{k}{K}, \frac{k'}{K}, g_{\text{rel}} \right) \right. \\ & \left. + \sum_{i=1}^n \sum_{k=0}^K \mathbf{w}_{\mathbf{u},ik} \log \mathbf{w}_{\mathbf{u},ik} + \sum_{j=1}^p \sum_{k=0}^K \mathbf{w}_{\mathbf{v},jk} \log \mathbf{w}_{\mathbf{v},jk} \right\}, \end{aligned}$$

with

$$\text{LSE}(X, \tau, Y, A, U, V, g_{\text{rel}}) := \log \int_0^1 \exp \left\{ -\frac{\tau}{2} (X - g_{\text{rel}}(Y, A, U, V, u))^2 \right\} du.$$

Weight updates are similar to those in EBMR–sep:

$$\mathbf{w}_{\mathbf{u},ik} \propto \exp \left(\sum_{j=1}^p \sum_{k'=0}^K \mathbf{w}_{\mathbf{v},jk'} \log \sum_{k''=0}^K \exp \left\{ -\frac{\tau_{ij}}{2} \left[x_{ij} - g_{\text{rel}}(y_i, a_j, \frac{k}{K}, \frac{k'}{K}, \frac{k''}{K}) \right]^2 \right\} \right), \quad (59)$$

$$\mathbf{w}_{\mathbf{v},jk} \propto \exp \left(\sum_{i=1}^n \sum_{k'=0}^K \mathbf{w}_{\mathbf{u},ik'} \log \sum_{k''=0}^K \exp \left\{ -\frac{\tau_{ij}}{2} \left[x_{ij} - g_{\text{rel}}(y_i, a_j, \frac{k'}{K}, \frac{k}{K}, \frac{k''}{K}) \right]^2 \right\} \right), \quad (60)$$

normalized to lie in Δ_{K+1} . With fixed weights, update g_{rel} by

$$\hat{g}_{\text{rel}} \in \arg \max_{g_{\text{rel}} \in \mathcal{G}_{\text{NN}}} \sum_{i=1}^n \sum_{j=1}^p \sum_{k=0}^K \sum_{k'=0}^K \mathbf{w}_{\mathbf{u},ik} \mathbf{w}_{\mathbf{v},jk'} \log \sum_{k''=0}^K \exp \left\{ -\frac{\tau_{ij}}{2} \left[x_{ij} - g_{\text{rel}}(y_i, a_j, \frac{k}{K}, \frac{k'}{K}, \frac{k''}{K}) \right]^2 \right\}. \quad (61)$$

The algorithm fits \hat{g}_{rel} by iterating steps (59)–(61) until convergence. With the estimate \hat{g}_{rel} , we sample from the posterior $p(z_{ij} | \hat{g}_{\text{rel}}, \mathbf{x}_{n,p})$ of model (57), given by

$$(u_i, u_j, u_{ij}) \sim p(u_i, u_j, u_{ij} | \hat{g}_{\text{rel}}, \mathbf{x}_{n,p}), \quad z_{ij} = \hat{g}_{\text{rel}}(u_i, u_j, u_{ij}). \quad (62)$$

E Algorithms for Empirical Bayes Spatial Regression

Recall that the invariant variable is the spectral density $\psi \in \mathcal{P}_{ac}(\mathbb{R}^d)$. Following [Wilson and Adams \(2013\)](#), we further parametrize ψ as a Gaussian mixture,

$$\psi_{\theta}(s) = \sum_{k=1}^K w_k \phi(s; \mu_k, \Sigma_k), \quad w_k \geq 0, \quad \sum_{k=1}^K w_k = 1, \quad (63)$$

where each $\Sigma_k = \text{diag}(\sigma_{k,1}^2, \dots, \sigma_{k,d}^2)$ is diagonal. By Bochner's theorem, Eq. 63 induces the kernel

$$k_{\theta}(\Delta) = \sum_{k=1}^K w_k \prod_{j=1}^d \cos(2\pi \mu_{k,j} \Delta_j) \exp(-2\pi^2 \sigma_{k,j}^2 \Delta_j^2), \quad (64)$$

for lags $\Delta \in \mathbb{R}^d$. The invariant variable is thus $\theta = (w_{1:K}, \mu_{1:K}, \Sigma_{1:K})$, which governs the stationary prior $\text{GP}(0, k_{\theta})$ for the latent process.

With this parametrization, the empirical Bayes spatial regression model is

$$\mathbf{z} \sim \text{GP}(0, k_{\theta}), \quad \beta \sim \pi(\beta) \propto 1, \quad x_{\omega} \sim \mathcal{N}(\beta^{\top} a_{\omega} + z_{\omega}, \tau_{\omega}^{-1}). \quad (65)$$

Posterior Inference. We estimate the kernel parameters θ by maximizing the marginal likelihood,

$$\hat{\theta} \in \arg \max_{\theta \in \Theta} \log \int \left[\prod_{\omega \in S_n} p(x_\omega | z_\omega, \beta) \right] p(z_n | \theta) \pi(\beta) d\beta dz_n. \quad (66)$$

This fits the spectral density (equivalently, the kernel) that best explains the marginal distribution of the observed spatial data. Given $\hat{\theta}$, the posterior $p(\beta, z_n | \mathbf{x}_n, \hat{\theta})$ is Gaussian with known mean and covariance.

Let $S_n = (\omega_1, \dots, \omega_n)$, $\mathbf{A}_n = [a_{\omega_1}, \dots, a_{\omega_n}]^\top \in \mathbb{R}^{n \times p}$, and $D_\tau = \text{diag}(\tau_{\omega_1}, \dots, \tau_{\omega_n})$. With $\Sigma_\theta = [k_\theta(\omega_i - \omega_j)]_{(i,j) \in [n]^2}$, define $S_\theta = \Sigma_\theta + D_\tau^{-1}$ and $W_\theta = S_\theta^{-1}$. Assuming \mathbf{A}_n has full column rank and $\pi(\beta) \equiv 1$, the MMLE objective is

$$\ell(\mathbf{x}_n; \theta) = \log \det S_\theta + \log |\mathbf{A}_n^\top W_\theta \mathbf{A}_n| + \mathbf{x}_n^\top W_\theta \mathbf{x}_n - \mathbf{x}_n^\top W_\theta \mathbf{A}_n \hat{\beta}_\theta, \quad (67)$$

where $\hat{\beta}_\theta = (\mathbf{A}_n^\top W_\theta \mathbf{A}_n)^{-1} \mathbf{A}_n^\top W_\theta \mathbf{x}_n$ is the weighted least-squares estimator.

We minimize (67) using stochastic gradient descent (Robbins and Monro, 1951). The computational bottleneck is to solve linear systems in S_θ ; we avoid forming W_θ explicitly by using a Cholesky factorization $S_\theta = LL^\top$. The resulting costs are $O(n^3)$ time and $O(n^2)$ space, which are tractable if the number of sites n is in the thousands. Scalable alternatives are available, including Nyström approximations and variational low-rank Gaussian processes (Hensman et al., 2013).

With $S_{\hat{\theta}} = \Sigma_{\hat{\theta}} + D_\tau^{-1}$, $W_{\hat{\theta}} = S_{\hat{\theta}}^{-1}$, and $\hat{\beta}_{\hat{\theta}} = (\mathbf{A}_n^\top W_{\hat{\theta}} \mathbf{A}_n)^{-1} \mathbf{A}_n^\top W_{\hat{\theta}} \mathbf{x}_n$,

$$\beta | \mathbf{x}_n \sim \mathcal{N} \left(\hat{\beta}_{\hat{\theta}}, (\mathbf{A}_n^\top W_{\hat{\theta}} \mathbf{A}_n)^{-1} \right), \quad (68)$$

and, conditional on β ,

$$z_n | \beta, \mathbf{x}_n \sim \mathcal{N} \left((\Sigma_{\hat{\theta}}^{-1} + D_\tau)^{-1} D_\tau (\mathbf{x}_n - \mathbf{A}_n \beta), (\Sigma_{\hat{\theta}}^{-1} + D_\tau)^{-1} \right). \quad (69)$$

Posterior samples are obtained by Monte Carlo: sample $\beta^{(s)}$ from (68), then $z_n^{(s)}$ from (69) with $\beta = \beta^{(s)}$.

Kriging. To predict at new sites $S'_n \supset S_n$, define $Q_\theta \in \mathbb{R}^{|S'_n| \times |S'_n|}$ by $Q_{\theta,ii} = [\Sigma_\theta^{-1}]_{ii} + \tau_i$ and $Q_{\theta,ij} = [\Sigma_\theta^{-1}]_{ij}$ for $i \neq j$, where τ_i denotes the noise precision at site ω_i . Let $L \in \mathbb{R}^{|S'_n|}$ have entries $L_{S_n} = D_\tau(\mathbf{x}_{S_n} - \mathbf{A}_{S_n} \beta)$ and zeros elsewhere. Then

$$z_{S'_n} | \beta, \mathbf{x}_n \sim \mathcal{N} \left(Q_{\hat{\theta}}^{-1} L, Q_{\hat{\theta}}^{-1} \right). \quad (70)$$

F Proofs

F.1 Proofs of § 2

Proof of Proposition 1 and Proposition 2. Let $S_n^c := \Omega \setminus S_n$. The true distribution $p^*(\mathbf{x}_n)$ is the S_n -marginal of $p^*(\mathbf{x})$:

$$p^*(\mathbf{x}_n) = \int p^*(\mathbf{x}) d\mathbf{x}_{S_n^c}.$$

By Assumption 1,

$$p^*(\mathbf{x}) = \int_{\mathcal{Z}^\Omega} p^*(\mathbf{z}) \prod_{\omega \in \Omega} p(x_\omega | z_\omega) d\mathbf{z}.$$

Applying Fubini's theorem to interchange the integrals over \mathbf{z} and $\mathbf{x}_{S_n^c}$ gives

$$\begin{aligned} p^*(\mathbf{x}_n) &= \int_{\mathcal{Z}^{S_n^c}} \int_{\mathcal{Z}^\Omega} p^*(\mathbf{z}) \prod_{\omega \in \Omega} p(x_\omega | z_\omega) d\mathbf{z} d\mathbf{x}_{S_n^c} \\ &= \int_{\mathcal{Z}^\Omega} p^*(\mathbf{z}) \prod_{\omega \in S_n} p(x_\omega | z_\omega) \left(\int_{\mathcal{Z}^{S_n^c}} \prod_{\omega \in S_n^c} p(x_\omega | z_\omega) d\mathbf{x}_{S_n^c} \right) d\mathbf{z} \\ &= \int_{\mathcal{Z}^\Omega} p^*(\mathbf{z}) \prod_{\omega \in S_n} p(x_\omega | z_\omega) d\mathbf{z}, \end{aligned}$$

which establishes Proposition 1.

For Proposition 2, we integrate the representation (10) over \mathbf{x}_{S_n} :

$$\begin{aligned} p^*(\mathbf{x}_n) &= \int_{\mathcal{Z}^{S_n}} \int_{\mathcal{G}} \left(\int_{\mathcal{Z}^{S_n^c}} p(\mathbf{z} | g) d\mathbf{z}_{S_n^c} \right) d\mu^*(g) \prod_{\omega \in S_n} p(x_\omega | z_\omega) d\mathbf{z}_{S_n} \\ &= \int_{\mathcal{Z}^{S_n}} \left(\int_{\mathcal{G}} p(\mathbf{z}_n | g) d\mu^*(g) \right) \prod_{\omega \in S_n} p(x_\omega | z_\omega) d\mathbf{z}_{S_n}. \end{aligned}$$

□

F.2 Proofs of the Algorithms

Proof of Eq. 44. For $q \in \mathcal{Q}_{\text{sep}}$ we can decompose the ELBO as

$$\begin{aligned} \text{ELBO} \left(q, g_{\text{sep}} \right) &= \sum_{i=1}^n \sum_{j=1}^p \mathbb{E}_{q_{\mathbf{u},i}(u_i) q_{\mathbf{v},j}(v_j)} \left[\mathbb{E}_{q_{ij}(u_{ij}|u_i, v_j)} \left[\log p(x_{ij} | g_{\text{sep}}(u_i, v_j, u_{ij})) \right] \right] \\ &\quad - \sum_{i=1}^n \mathbb{E}_{q_{\mathbf{u},i}(u_i)} [\log q_{\mathbf{u},i}(u_i)] - \sum_{j=1}^p \mathbb{E}_{q_{\mathbf{v},j}(v_j)} [\log q_{\mathbf{v},j}(v_j)] \\ &\quad - \sum_{i=1}^n \sum_{j=1}^p \mathbb{E}_{q_{\mathbf{u},i}(u_i) q_{\mathbf{v},j}(v_j)} \left[\mathbb{E}_{q_{ij}(u_{ij}|u_i, v_j)} [\log q_{ij}(u_{ij} | u_i, v_j)] \right]. \end{aligned}$$

Introduce the reference distribution

$$q_{\text{ref}}(u_{ij} | u_i, v_j) \propto \exp \left\{ -\frac{\tau_{ij}}{2} (x_{ij} - g_{\text{sep}}(u_i, v_j, u_{ij}))^2 \right\}.$$

Then

$$\begin{aligned} \text{ELBO} \left(q, g_{\text{sep}} \right) &= \sum_{i=1}^n \sum_{j=1}^p \mathbb{E}_{q_{\mathbf{u},i}(u_i) q_{\mathbf{v},j}(v_j)} \left[\text{LSE}(x_{ij}, \tau_{ij}, u_i, v_j, g_{\text{sep}}) \right] \\ &\quad - \sum_{i=1}^n \mathbb{E}_{q_{\mathbf{u},i}(u_i)} [\log q_{\mathbf{u},i}(u_i)] - \sum_{j=1}^p \mathbb{E}_{q_{\mathbf{v},j}(v_j)} [\log q_{\mathbf{v},j}(v_j)] \\ &\quad - \sum_{i=1}^n \sum_{j=1}^p \mathbb{E}_{q_{\mathbf{u},i}(u_i) q_{\mathbf{v},j}(v_j)} \left[D_{\text{KL}} (q_{ij}(\cdot | u_i, v_j) \| q_{\text{ref}}(\cdot | u_i, v_j)) \right], \end{aligned} \tag{71}$$

where

$$\text{LSE}(X, \tau, U, V, g_{\text{sep}}) := \log \int_0^1 \exp \left\{ -\frac{\tau}{2} [X - g_{\text{sep}}(U, V, u)]^2 \right\} du.$$

Maximizing over q_{ij} for fixed $q_{\mathbf{u}}, q_{\mathbf{v}}$ gives

$$q_{ij}^*(u_{ij} | u_i, v_j) = q_{\text{ref}}(u_{ij} | u_i, v_j),$$

and evaluating at q^* yields

$$\begin{aligned} \text{ELBO} \left(q^*, g_{\text{sep}} \right) &= \sum_{i=1}^n \sum_{j=1}^p \mathbb{E}_{q_{\mathbf{u},i}^*(u_i) q_{\mathbf{v},j}^*(v_j)} \left[\text{LSE}(x_{ij}, \tau_{ij}, u_i, v_j, g_{\text{sep}}) \right] \\ &\quad - \sum_{i=1}^n \mathbb{E}_{q_{\mathbf{u},i}^*(u_i)} [\log q_{\mathbf{u},i}^*(u_i)] - \sum_{j=1}^p \mathbb{E}_{q_{\mathbf{v},j}^*(v_j)} [\log q_{\mathbf{v},j}^*(v_j)]. \end{aligned}$$

□

Proof of Proposition 4. Recall that $u_k = k/K$ for $k = 0, \dots, K$. The discretized form of (44) is

$$\begin{aligned} \hat{g}_{\text{sep}} \in \arg \max_{g_{\text{sep}} \in \mathcal{G}_{\text{NN}}} \sup_{\mathbf{w} \in \Delta_{K+1}^{n+p}} & \left\{ \sum_{i=1}^n \sum_{j=1}^p \sum_{k_1=0}^K \sum_{k_2=0}^K w_{\mathbf{u},ik_1} w_{\mathbf{v},jk_2} \widehat{\text{LSE}}(x_{ij}, \tau_{ij}, u_{k_1}, u_{k_2}, g_{\text{sep}}) \right. \\ & \left. - \sum_{i=1}^n \sum_{k=0}^K w_{\mathbf{u},ik} \log w_{\mathbf{u},ik} - \sum_{j=1}^p \sum_{k=0}^K w_{\mathbf{v},jk} \log w_{\mathbf{v},jk} \right\}, \end{aligned} \quad (72)$$

where \mathbf{w} collects all weight vectors $\mathbf{w}_{\mathbf{u},1}, \dots, \mathbf{w}_{\mathbf{u},n}, \mathbf{w}_{\mathbf{v},1}, \dots, \mathbf{w}_{\mathbf{v},p}$ and $\widehat{\text{LSE}}$ is the discretized form of LSE .

We fit $\mathbf{w}_{\mathbf{u}}, \mathbf{w}_{\mathbf{v}}$ and g_{sep} by alternating updates. For $j \in [p]$ and $k = 0, \dots, K$,

$$w_{\mathbf{v},jk} = \frac{\exp \left(\sum_{i=1}^n \sum_{k_1=0}^K w_{\mathbf{u},ik_1} \widehat{\text{LSE}}(x_{ij}, \tau_{ij}, u_{k_1}, u_k, g_{\text{sep}}) \right)}{\sum_{k'=0}^K \exp \left(\sum_{i=1}^n \sum_{k_1=0}^K w_{\mathbf{u},ik_1} \widehat{\text{LSE}}(x_{ij}, \tau_{ij}, u_{k_1}, u_{k'}, g_{\text{sep}}) \right)}. \quad (73)$$

Similarly, for $i \in [n]$ and $k = 0, \dots, K$,

$$w_{\mathbf{u},ik} = \frac{\exp \left(\sum_{j=1}^p \sum_{k_2=0}^K w_{\mathbf{v},jk_2} \widehat{\text{LSE}}(x_{ij}, \tau_{ij}, u_k, u_{k_2}, g_{\text{sep}}) \right)}{\sum_{k'=0}^K \exp \left(\sum_{j=1}^p \sum_{k_2=0}^K w_{\mathbf{v},jk_2} \widehat{\text{LSE}}(x_{ij}, \tau_{ij}, u_k, u_{k'}, g_{\text{sep}}) \right)}. \quad (74)$$

Finally, we train the neural network g_{sep} by maximizing the weighted objective

$$g_{\text{sep}} \in \arg \max_{g_{\text{sep}} \in \mathcal{G}_{\text{NN}}} \sum_{i=1}^n \sum_{j=1}^p \sum_{k_1=0}^K \sum_{k_2=0}^K w_{\mathbf{u},ik_1} w_{\mathbf{v},jk_2} \widehat{\text{LSE}}(x_{ij}, \tau_{ij}, u_{k_1}, u_{k_2}, g_{\text{sep}}). \quad (75)$$

□

Proof of Proposition 5. By the Gibbs variational principle,

$$\log p(\mathbf{x}_n | \mathbf{g}_{\text{joint}}) = \sup_{\mathbf{q} \in \mathcal{P}([0,1]^{n+n^2})} \left\{ \sum_{i=1}^n \sum_{j=1}^n \mathbb{E}_{\mathbf{q}(u_i, u_j, u_{ij})} [\log p(x_{ij} | \mathbf{g}_{\text{joint}}(u_i, u_j, u_{ij}))] - \mathbb{E}_{\mathbf{q}(\mathbf{u}_n)} [\log \mathbf{q}(\mathbf{u}_n)] \right\}. \quad (76)$$

Leveraging the structure of $\mathbf{q} \in \mathcal{Q}$ and rearranging yields

$$\text{ELBO} = \sup_{\mathbf{q} \in \mathcal{Q}} \left\{ - \sum_{i=1}^n \sum_{j=1}^n \mathbb{E}_{\mathbf{q}_{\mathbf{u},i}(u_i) \mathbf{q}_{\mathbf{u},j}(u_j)} [D_{\text{KL}}(\mathbf{q}_{ij}(\cdot | u_i, u_j) \| \mathbf{q}_{\text{ref}}(\cdot | u_i, u_j))] - \sum_{i=1}^n \mathbb{E}_{\mathbf{q}_{\mathbf{u},i}(u_i)} [\log \mathbf{q}_{\mathbf{u},i}(u_i)] \right\},$$

where $\mathbf{q}_{\text{ref}}(u_{ij} | u_i, u_j) \propto \exp\left(-\frac{\tau_{ij}}{2} [x_{ij} - \mathbf{g}_{\text{joint}}(u_i, u_j, u_{ij})]^2\right)$. Then, maximizing the ELBO over \mathbf{q}_{ij} for fixed $\mathbf{q}_{\mathbf{u}}$ yields the stated objective. \square

Proof of Eq. 67. Integrating over $\mathbf{z}_n \sim \mathcal{N}(0, \Sigma_{\theta})$ gives

$$\mathbf{x}_n | \beta, \theta \sim \mathcal{N}(\mathbf{A}_n \beta, S_{\theta}).$$

With $\pi(\beta) \equiv 1$, integrating over β yields

$$\log p(\mathbf{x}_n | \theta) = -\frac{1}{2} \left\{ \log \det S_{\theta} + \log |\mathbf{A}_n^{\top} W_{\theta} \mathbf{A}_n| + (\mathbf{x}_n - \mathbf{A}_n \hat{\beta}_{\theta})^{\top} W_{\theta} (\mathbf{x}_n - \mathbf{A}_n \hat{\beta}_{\theta}) \right\} + C,$$

where C is constant in θ . The objective $\ell(\mathbf{x}_n; \theta)$ equals $-\log p(\mathbf{x}_n | \theta)$ up to an additive constant. \square

Proof of Corollary 1. The discretized version of (54) is

$$\sup_{\mathbf{w} \in \Delta_{K+1}^n} \sup_{\mathbf{g}_{\text{joint}} \in \mathcal{G}_{\text{NN}}} \sum_{i=1}^n \sum_{k=0}^K w_{ik} \left[\widehat{\text{LSE}}(x_{ii}, \tau_{ii}, u_k, u_k, \mathbf{g}_{\text{joint}}) + \sum_{j \neq i} \sum_{k_2=0}^K w_{jk_2} \widehat{\text{LSE}}(x_{ij}, \tau_{ij}, u_k, u_{k_2}, \mathbf{g}_{\text{joint}}) - \log w_{ik} \right],$$

where

$$\widehat{\text{LSE}}(x_{ij}, \tau_{ij}, u_i, u_j, \mathbf{g}_{\text{joint}}) := \log \sum_{k=0}^K \exp\left(-\frac{\tau_{ij}}{2} [x_{ij} - \mathbf{g}_{\text{joint}}(u_i, u_j, u_k)]^2\right) - \log(K+1).$$

Alternating maximization over \mathbf{w} (softmax updates) and over $\mathbf{g}_{\text{joint}}$ (stochastic gradient step) yields the stated algorithm. \square

Proof of Eq. 70. Conditional on β , the joint model for $\mathbf{z}_{S'_n}$ and \mathbf{x}_{S_n} is

$$\mathbf{z}_{S'_n} \sim \mathcal{N}(0, \Sigma_{\hat{\theta}}), \quad \mathbf{x}_{S_n} \sim \mathcal{N}(\mathbf{A}_{S_n} \beta + \mathbf{z}_{S_n}, D_{\tau}^{-1}).$$

By Bayes' rule,

$$\begin{aligned} p(\mathbf{z}_{S'_n} | \mathbf{x}_{S_n}, \beta) &\propto \exp\left(-\frac{1}{2} \mathbf{z}_{S'_n}^{\top} \Sigma_{\hat{\theta}}^{-1} \mathbf{z}_{S'_n} - \frac{1}{2} (\mathbf{x}_{S_n} - \mathbf{A}_{S_n} \beta - \mathbf{z}_{S_n})^{\top} D_{\tau} (\mathbf{x}_{S_n} - \mathbf{A}_{S_n} \beta - \mathbf{z}_{S_n})\right) \\ &\propto \exp\left(-\frac{1}{2} \mathbf{z}_{S'_n}^{\top} Q_{\hat{\theta}} \mathbf{z}_{S'_n} + \mathbf{z}_{S'_n}^{\top} L\right), \end{aligned}$$

where $Q_{\hat{\theta}}$ and L are defined in the main text. Hence the posterior is Gaussian with mean $Q_{\hat{\theta}}^{-1} L$ and covariance $Q_{\hat{\theta}}^{-1}$. \square

Table 3: Comparison of matrix-recovery performance for NPMLE, EBMR–Sep, and EBMF across generating functions. We report the mean and standard error of R-MSE. The lowest R-MSE in each scenario is shown in **bold**.

n	p	τ	Linear			Sine-log			Sine-cos		
			NPMLE	EBMR-Sep	EBMF	NPMLE	EBMR-Sep	EBMF	NPMLE	EBMR-Sep	EBMF
20	20	0.1	3.81 (0.48)	3.54 (0.38)	12.27 (2.23)	2.55 (0.47)	2.13 (0.29)	9.24 (0.00)	3.30 (0.43)	2.69 (0.41)	2.14 (0.00)
20	20	0.25	7.30 (0.22)	6.35 (0.35)	10.61 (0.40)	4.18 (0.23)	3.73 (0.21)	11.18 (1.38)	5.94 (0.27)	4.71 (0.30)	5.36 (0.00)
20	20	1	23.13 (0.57)	15.87 (0.72)	18.33 (0.50)	13.35 (0.39)	12.19 (0.66)	14.84 (0.48)	18.80 (0.34)	10.98 (1.41)	10.69 (1.29)
20	20	4	53.01 (1.28)	34.17 (0.65)	44.63 (0.78)	36.87 (0.96)	26.75 (0.80)	32.18 (0.75)	48.46 (0.91)	22.58 (7.24)	13.35 (0.71)
20	50	0.1	2.88 (0.08)	2.74 (0.17)	8.44 (0.30)	1.94 (0.07)	1.91 (0.16)	9.56 (0.55)	2.42 (0.09)	2.45 (0.22)	2.06 (0.00)
20	50	0.25	6.36 (0.08)	5.18 (0.18)	9.94 (0.31)	4.17 (0.08)	3.73 (0.25)	8.39 (0.23)	5.43 (0.11)	3.61 (0.29)	5.14 (0.00)
20	50	1	20.38 (0.21)	13.47 (1.29)	22.77 (0.38)	14.07 (0.16)	9.76 (0.65)	18.05 (0.42)	17.86 (0.21)	6.39 (0.42)	20.55 (0.00)
20	50	4	50.17 (0.67)	36.63 (6.97)	69.41 (0.23)	38.73 (0.51)	22.32 (0.47)	49.97 (0.22)	44.45 (0.51)	8.97 (0.55)	37.90 (1.30)
50	50	0.1	2.73 (0.06)	2.23 (0.04)	4.63 (0.14)	1.73 (0.06)	1.49 (0.05)	3.93 (0.15)	1.94 (0.05)	1.30 (0.10)	1.84 (0.00)
50	50	0.25	6.33 (0.09)	4.36 (0.12)	5.89 (0.15)	3.98 (0.08)	3.02 (0.07)	4.95 (0.14)	4.60 (0.09)	2.46 (0.37)	4.63 (0.22)
50	50	1	20.83 (0.14)	10.66 (0.16)	12.24 (0.18)	13.67 (0.11)	7.54 (0.16)	8.57 (0.18)	15.73 (0.09)	4.26 (1.56)	4.59 (0.17)
50	50	4	51.34 (0.50)	28.38 (0.30)	37.47 (0.30)	38.42 (0.31)	19.70 (0.18)	23.19 (0.28)	42.61 (0.37)	4.88 (0.27)	6.39 (0.24)
n	p	τ	Tanh			Reciprocal					
			NPMLE	EBMR-Sep	EBMF	NPMLE	EBMR-Sep	EBMF			
20	20	0.1	1.45 (0.40)	1.06 (0.33)	7.57 (0.00)	1.36 (0.38)	1.02 (0.36)	1.84 (0.00)			
20	20	0.25	1.25 (0.26)	0.79 (0.14)	11.35 (1.68)	1.14 (0.26)	1.36 (0.72)	4.61 (0.00)			
20	20	1	2.81 (0.21)	2.64 (0.33)	10.16 (0.50)	1.84 (0.16)	1.92 (0.34)	12.46 (1.66)			
20	20	4	8.99 (0.65)	7.14 (0.51)	14.49 (0.95)	5.26 (0.49)	4.54 (0.33)	12.04 (0.71)			
20	50	0.1	0.59 (0.07)	0.56 (0.13)	7.47 (0.28)	0.57 (0.07)	0.58 (0.13)	1.75 (0.00)			
20	50	0.25	0.94 (0.09)	0.54 (0.07)	5.75 (0.19)	0.78 (0.12)	0.41 (0.09)	4.38 (0.00)			
20	50	1	2.13 (0.20)	1.75 (0.18)	8.07 (0.41)	1.62 (0.19)	1.11 (0.16)	8.16 (1.10)			
20	50	4	5.60 (0.11)	4.88 (0.13)	10.65 (0.21)	3.18 (0.06)	3.14 (0.14)	9.01 (0.18)			
50	50	0.1	0.41 (0.05)	0.32 (0.04)	3.91 (0.41)	0.29 (0.06)	0.25 (0.05)	2.14 (0.19)			
50	50	0.25	0.77 (0.08)	0.60 (0.02)	3.91 (0.14)	0.50 (0.09)	0.34 (0.03)	4.21 (0.28)			
50	50	1	2.31 (0.06)	2.01 (0.04)	4.85 (0.18)	1.23 (0.03)	1.01 (0.02)	4.13 (0.15)			
50	50	4	8.07 (0.06)	5.78 (0.13)	7.87 (0.30)	4.07 (0.06)	3.43 (0.12)	5.23 (0.31)			

G Additional Empirical Results

G.1 Matrix Recovery Results

Table 3 reports the empirical Bayes matrix recovery results across all simulation settings described in § 4.1.

G.2 Covariate-Assisted Empirical Bayes with Model Misspecification

To assess the robustness of Bayesian EB methods, we compare covariate-assisted empirical Bayes to competing methods under a heavy-tailed noise. For each (n, p, T_0) design, we generate independent noise ε_{ij} from a scaled Student- t distribution with $v = 5$ degrees of freedom:

$$\varepsilon_{ij} \sim c_v t_v, \quad c_v = \frac{\sigma}{\sqrt{v/(v-2)}},$$

where c_v is chosen to ensure $\text{Var}(\varepsilon_{ij}) = \sigma^2$. Thus, the noise variance matches the target variance but the tail probabilities are heavier than Gaussian.

Figure 8 plots RMSE of $\hat{z}_{n,p}$ versus p ; points show medians across replicates and bands indicate interquartile ranges for each method.

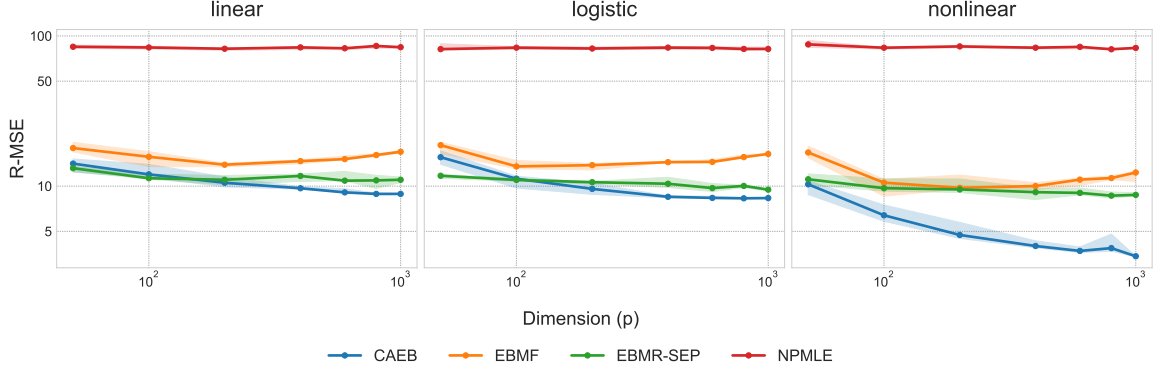


Figure 8: CAEB under heavy-tailed noise. R-MSE of latent recovery versus dimension p for three choices of g : linear, logistic, and nonlinear. Curves compare CAEB, EBMF, EBMR-*sep*, and NPMLE; points are medians and bands are IQR (25–75%). With noise following a t_5 distribution, CAEB attains the lowest error and continues to improve as the number of columns p increases.

G.3 Empirical Bayes Spatial Regression Results

Figure 9 shows that the MSE of the posterior mean estimator of β relative to β^* decreases as the sample size n grows, for different choices of the number of spectral mixture components K .

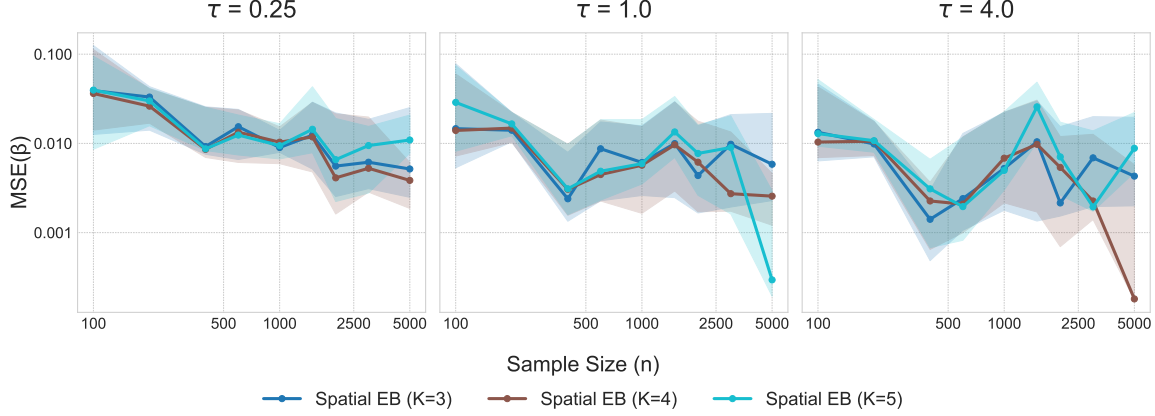


Figure 9: Posterior mean estimation of β^* improves with increasing n . Mean squared error (MSE) for estimating β^* using the posterior mean under the EB spatial regression, across varying sample size n and precision τ . We fit the spectral density using $K \in \{3, 4, 5\}$ Gaussian components; results are robust to moderate over-specification of K . Both axes use logarithmic scales. The points denote medians over 10 replicates, while bands show interquartile ranges (25–75%).

G.4 Additional Results for NYC Air Quality

Fitted Spectral Density

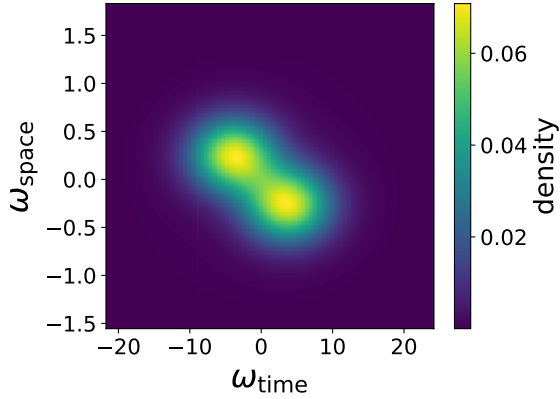


Figure 10: Fitted spectral density for weekly PM_{2.5} in New York City, with $K = 10$. The spectrum shows two dominant modes—one on the upper left corner and one on the lower right corner, which indicates two distinct spatio–temporal regimes. Based on the denoised series and site geography, one mode might correspond to the Manhattan sites (Herald Square, Chinatown, Lower East Side) and the other might correspond to northern Queens.

Posterior Marginals of β

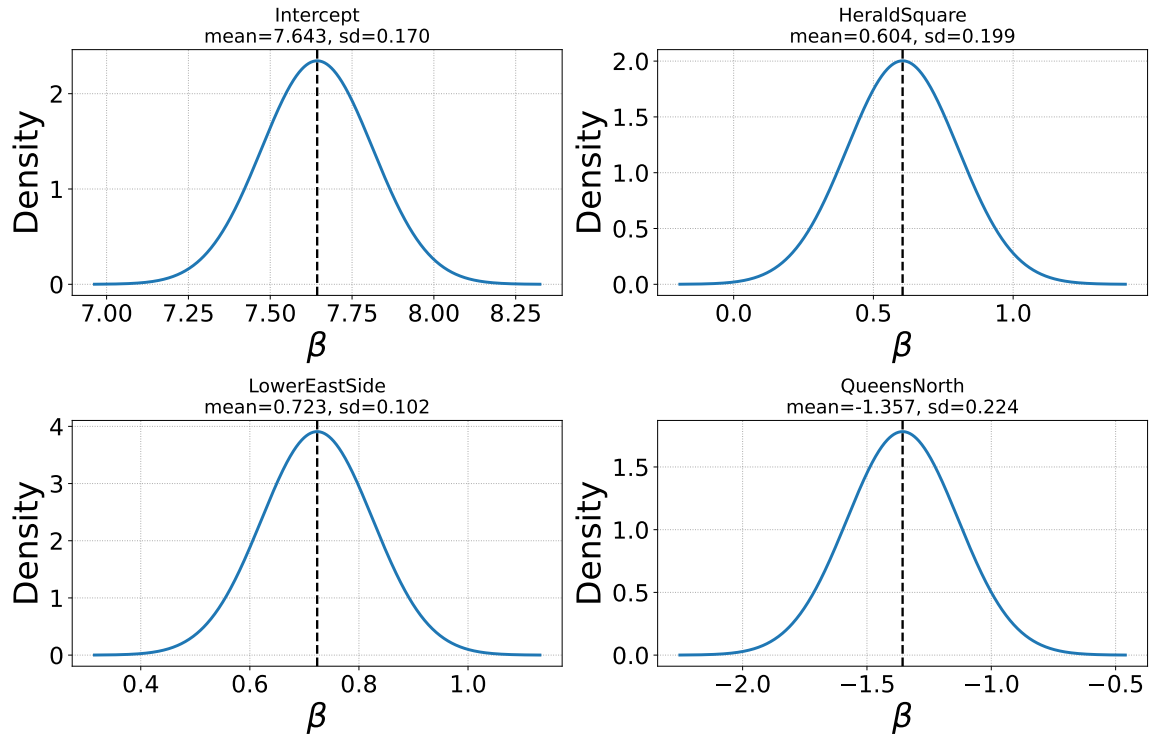


Figure 11: Posterior distributions of location effects in EB spatial regression for NYC PM_{2.5}. Baseline is Herald Square (the mean is $7.654 \mu\text{g}/\text{m}^3$). The effect of measuring at Lower East Side is statistically indistinguishable from the baseline. Queens North is lower by $1.357 \mu\text{g}/\text{m}^3$ (posterior s.d. 0.224), which provides strong evidence of better air quality there relative to Herald Square.